LA-UR-16-28290
Approved for public release; distribution is unlimited.

Title: Nondestructive Assay Data Integration with the SKB-50 Assemblies - FY16 Update

Author(s): Tobin, Stephen Joseph; Fugate, Michael Lynn; Trellue, Holly Renee; DeBaere, Paul; Sjoland, Anders; Liljenfeldt, Henrik; Hu, Jianwei; Backstrom, Ulrika; Bengtsson, Martin; Burr, Tomas; Eliasson, Annika; Favalli, Andrea; Gauld, Ian; Grogan, Brandon; Jansson, Peter; Junell, Henrik; Schwalbach, Peter; Vaccaro, Stefano; Vo, Duc Ta; Wildestrand, Henrik

Intended for: Report

Issued: 2016-10-28

Nondestructive Assay Data Integration with the SKB-50 Assemblies - FY16 Update

S.J. Tobin[1], M.L. Fugate[1], H.R. Trellue[1], P. De-Baere[2], A. Sjöland[3], H. Liljenfeldt[4], J. Hu[4], U. Bäckström[3,5], M. Bengtsson[3,5], T. Burr[1,6], A. Eliasson[3], A. Favalli[1], I. Gauld[4], B. Grogan[4], P. Jansson[7], H. Junéll[3], P. Schwalbach[2], S. Vaccaro[2], D. Vo[1], and H. Wildestrand[3,5]

[1]Los Alamos National Laboratory, USA

[2]DG Energy, Directorate Nuclear Safeguards, Luxembourg

[3]Swedish Nuclear Fuel and Waste Management Company, Sweden

[4]Oak Ridge National Laboratory, USA

[5]Vattenfall AB, Sweden

[6]International Atomic Energy Agency, Austria

[7]Uppsala University, Sweden

October 21, 2016

1 Introduction

A project to research the application of non-destructive assay (NDA) techniques for spent fuel assemblies is underway at the Central Interim Storage Facility for Spent Nuclear Fuel (for which the Swedish acronym is Clab) in Oskarshamn, Sweden. The project currently is a collaboration among the European Commission, DG Energy, Directorate Nuclear Safeguards (Euratom); the Swedish Nuclear Fuel and Waste Management Company (SKB); Oak Ridge National Laboratory; Vattenfall AB; International Atomic Energy Agency; Uppsala University; and Los Alamos National Laboratory participating in what was formerly known as the Next Generation Safeguards Initiative Spent Fuel (NGSI-SF) Project[1] [2] but is currently know as the NDA Spent Fuel Project (NDA-SF).

The research goals of this project contain both safeguards and non-safeguards interests. These non-destructive assay (NDA) technologies are designed to strengthen the technical toolkit of safeguard inspectors and others to determine the following technical goals more accurately:

1. Verify initial enrichment, burnup, and cooling time of facility declaration for spent fuel assemblies.
2. Detect replaced or missing pins from a given spent fuel assembly to confirm its integrity.
3. Estimate plutonium mass and related plutonium and uranium fissile mass parameters in spent fuel assemblies. Estimate heat content, and measure reactivity (multiplication).

Furthermore, the interests of SKB and/or Swedish domestic regulations motivate the inclusion of additional goals: (4) accurately estimate the heat content in each individual assembly in a rapid manner and (5) measure the reactivity of each assembly in order to assure all potential fuel configurations are safe.

Combining these research goals with the practical need to deploy robust hardware capable of measuring the NDA information emitted by spent fuel assemblies, the research team decided that the eventual NDA system(s), either used by the inspectorate and/or SKB, are anticipated to include spectral resolved passive gamma and total neutron measurement capabilities. Building upon this base NDA system, **the main research question involves quantifying what might be gained by adding additional NDA**

capability and what approach should be taken to access the usefulness of any such additional NDA capability.

Leveraging the research performed as part of the NGSI-SF Project, the research team and sponsors decided to deploy two advanced neutron based NDA instruments at Clab, each of the two instruments is capable of testing two unique NDA techniques. One instrument is passive and one utilizes an active neutron source; both are described in more detail later in this report. With respect to the experimental approach for accessing the usefulness of additional NDA capability, the research team decided to measure 50 assemblies with diverse characteristics in terms of the initial enrichment, burnup and cooling that were irradiated in both pressurized water reactors (PWR) and boiling water reactors (BWR).

The research team is currently in the early phases of analyzing the passive gamma and total neutron data obtained with a Fork [3][4] detector as well as spectral resolved data taken with a HPGe detector provided by Euratom. The NDA signal integration research conducted with simulated data as part of the NGSI-SF Project [5][6][7] motivated the application of pattern recognition techniques, often called Data Mining techniques as a means of producing useful information in the context of the various technical goals.

The reasons for measuring spent fuel assemblies with NDA are different among the parties that may use the results. An international safeguards inspectorate may differ from the State regulator or SKB in terms of what declared information they are willing to trust. All parties would prefer that an NDA analysis alone might meet their needs but some parties may be willing to use some declared values if the ability to estimate useful parameters is significantly improved. Or some of the stake holders might be willing to use a declared value after a given quantity is verified within a given tolerance by measurements. In light of this reality, a systematic approach to the use of declared values in the analysis is planned.

The analysis approach used in this report is the following: (1) Illustrate the NDA signals both relative to other NDA signals and relative to the parameters that are to be predicted. (2) Compare the measured results to commonly observed scaling factors along with simulated results. (3) As needed, include simulated results to expand *beyond* the experimental parameter space. (4) Data Mining techniques will be applied depending on available data and the complexity of the integration.

2 Non-destructive Assay Techniques

The NDA techniques deployed, or to be deployed, at Clab include five passive and two active NDA techniques. The passive techniques are the following: (1) Gross, or total, and spectral resolved gamma-ray emission detected with an ion chamber and a HPGe detector, respectively. The HPGe measurements used a collimated structure built into the pool wall that provided a direct line-of-sight view between a 15 mm vertical extent of the spent fuel assembly and the detector crystal. The assembly was measured with the fuel moving vertically in front of the collimator as well as with the assembly in a static position. These measurements were made with each of the 4 corners of the fuel pointed toward the HPGe detector[8][9][10][11][12][13][14]; the summation of the photons measured from the 4 different views of the assembly provided a nearly uniform assembly average emission. (2) The time correlated passive neutron emission will be detected with 56 ^{3}He tubes. Differential Die-away Self Interrogation (DDSI) analysis, which involves analyzing not only the traditional doubles count rates but variation among correlated neutrons measured during different time intervals following a detected trigger neutron, will be used [15][16][17]. (3) The total passive neutron emission will also be detected with DDSI and other instruments. The total neutron emission is listed separately here in recognition of the unique physics that this signal contains. (4) The DDSI hardware can be used for the deployment of the Passive Neutron Albedo Reactivity (PNAR) technique, though much simpler hardware could be used. The PNAR technique involves comparing the neutron count rate measured when the assembly is in both a high and low multiplying geometry [18][19][20][21]. The change in multiplication is achieved by measuring the assembly twice with two different steel liners. In one case the liner has 1 mmof Cd inside it and in the other case the Cd is absent. Both liners fit within the DDSI setup. Note that the PNAR techniques could be deployed with the two sections located one above the other; hence, avoiding the need for two measurements. (5) The total heat will be measured with an approximately 4 meter long calorimeter provided by SKB that is already installed at Clab [22][23]. The calorimeter was included in the NDA research mix to measure heat in fulfillment of domestic regulation. Yet, the availability of a calorimeter, both in this experimental phase and possibly at an encapsulation facility, provides an unique NDA signature that may have interesting potential to advance safeguards goals, particularly in the context of anomaly resolution.

The active interrogation instruments are the following: (6) The Differential Die-away (DDA) technique

[24][25][26] involves the measurement of the neutron intensity as a function of time following a 50 μs burst of neutrons; both the die-away time of the neutron population as well as the neutron count rate are measured. A deuterium-tritium (DT) neutron generator produces the neutron burst on one side of the assembly while neutron detectors that only detect neutrons with an energy above 0.5 eV surround the assembly on the other three sides. (7) The Californium Interrogation Prompt Neutron (CIPN) [27][28] technique will be tested with the hardware that was primarily designed for DDA by simply keeping the neutron generator on continuously for several seconds. With CIPN, the signal of interest is the difference between (a) the steady-state passive background count rate measured while the DT generator is turned off, and (b) the steady-state count rate that exists while the generator is on.

Two additional NDA deployments have or will also be used to measure the SKB-50 assemblies: (1) A Fork detector was deployed by Euratom. Although the total neutron and gross gamma signatures detected by an actual Fork detector will also be detected by the NDA instruments described previously, it is of interest to measure these signatures with the exact hardware commonly used in safeguards for both quality control reasons and systematic uncertainty quantification reasons. Furthermore, the only neutron data available at this time was measured with a Fork detector by Euratom. (2) A Digital Cerenkov Viewing Device (DCVD) [29][30], which measures the intensity and patterns of the Cerenkov light emitted from the water within the assembly, will also be deployed. Signatures from the DCVD measurement may be used in future analysis.

3 Diverse Fuel Assemblies Measured - the SKB-50

The Swedish Central Interim Storage Facility for Spent Nuclear Fuel, known by the Swedish acronym of "Clab," has an extensive variety of fuel from the 12 commercial reactors that have operated in Sweden, providing an ideal source of diverse fuels for experimental use. From among these tens of thousands of assemblies, 50 assemblies were selected that roughly span the diversity of fuel to be interred in the Swedish repository. Of these 50, 25 PWR assemblies were selected with initial enrichment values that span from 2.1% to 4.1%, burnup values that span from 20 to 53 GWd/tU and cooling time values that span from 5 to 30 years; 20 of the PWRs are 17x17 while 5 are 15x15. See Table 1 for more details on the PWR assemblies. Of

the 25 boiling water reactor (BWR) assemblies selected, initial enrichment spans from 1.3% to 4.0%, burnup spans from 9 to 46 GWd/tU and cooling time spans from 7 to 27 years; furthermore, the 25 BWR assemblies are comprised of 6 different commercial assembly types, hence there will be some geometric variation among them. Of particular note there are 11 8x8 assemblies and 14 10x10 assemblies. See Table 2 for more details on the BWR assemblies. The interpretation of the signals measured from this broad diversity of fuel will test the capability of the NDA techniques, as well as data integration and analysis.

For the PWR and BWR assemblies in the SKB-50, the variation of burnup with initial enrichment is illustrated in Figure 1; the burnup was calculated by the reactor operator. The primary factor normally influencing the shape of the initial enrichment vs. burnup graph is the desire of reactor operators to optimally consume the nuclear potential energy of each assembly [13]. In other words, if a reactor operator decides to pay for an elevated initial enrichment, they will generally want to irradiate the fuel to the optimum level to extract the electrical energy equivalent of their investment. There will naturally be some scatter in this optimization. Because we wanted to test our NDA instruments and analysis with a sampling of assemblies representing the breadth of fuel that would be measured, we intentionally selected more of the assemblies that were either under-irradiated or over-irradiated relative to how many would have been selected if a random sampling of assemblies were performed.

Table 1: PWR Assemblies for January 1, 2015

Assemby ID	Assembly Symbol	Initial Enrichment (wt %)	Burnup (GWd/tU)	Cooling Time (years)
PWR1	A	4.10	52.6	5.6
PWR2	B	3.93	49.6	5.6
PWR3	C	3.69	48.2	14.5
PWR4	D	3.93	46.9	6.6
PWR5	E	3.94	46.9	6.6
PWR6	F	3.60	45.7	15.5
PWR7	G	3.94	44.5	7.5
PWR8	H	3.30	44.4	26.3
PWR9	I	3.71	45.8	7.4
PWR10	J	3.70	43.5	16.5
PWR11	K	3.51	43.2	14.5
PWR12	L	3.30	43.0	26.3
PWR13	M	3.20	40.9	27.7
PWR14	N	3.51	40.8	17.5
PWR15	O	2.80	40.5	27.3
PWR16	P	3.60	40.4	18.5
PWR17	Q	3.70	40.3	15.3
PWR18	R	3.52	39.8	19.6
PWR19	S	3.20	35.0	29.7
PWR20	T	3.10	34.0	28.5
PWR21	U	3.10	34.0	28.5
PWR22	V	2.80	31.2	28.4
PWR23	W	3.60	28.5	18.5
PWR24	X	2.10	23.2	19.6
PWR25	Y	2.10	19.6	30.6

Table 2: BWR Assemblies for January 1, 2015

Assemby ID	Assembly Symbol	Initial Enrichment (wt %)	Burnup (GWd/tU)	Cooling Time (years)
BWR1	a	4.01	46.4	8.3
BWR2	b	3.20	43.8	10.4
BWR3	c	3.40	44.4	12.4
BWR4	d	3.40	41.9	12.4
BWR5	e	3.14	42	8.3
BWR6	f	2.65	38	29.3
BWR7	g	3.15	41.2	10.4
BWR8	h	3.15	39.8	9.6
BWR9	i	4.01	40.4	7.3
BWR10	j	3.14	39.5	8.3
BWR11	k	2.09	31.5	22.4
BWR12	l	2.96	33.5	9.6
BWR13	m	2.96	36.8	9.6
BWR14	n	2.65	30.4	29.3
BWR15	o	2.09	29.4	25.4
BWR16	p	2.09	26.8	27.6
BWR17	q	2.31	32.7	28.5
BWR18	r	2.09	21.5	22.4
BWR19	s	2.58	30.8	25.6
BWR20	t	2.96	26.4	9.6
BWR21	u	2.31	27.7	27.5
BWR22	v	2.96	20.4	9.6
BWR23	w	2.96	16.0	9.6
BWR24	x	1.27	13.3	27.5
BWR25	y	1.27	9.13	27.5

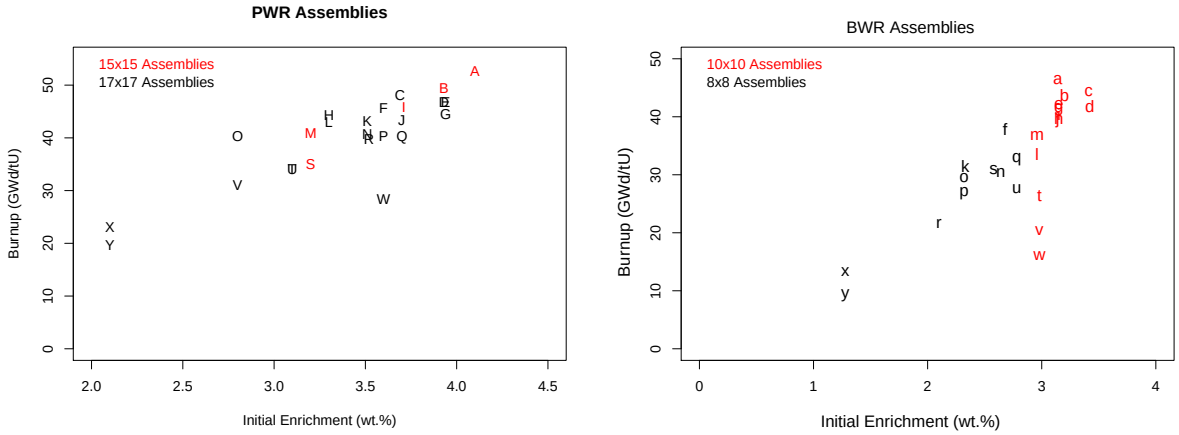

Figure 1: The burnup of the 25 PWR and 25 BWR assemblies are graphed as a function of their initial enrichment. Color is used to separate among the different assemblies types. Capital letters of the alphabet are used to indicate PWR assemblies consistent with Table 1, while minuscule letters of the alphabet are used to indicate BWR assemblies consistent with Table 2.

Figure 2 is included to illustrate that the PWR and BWR assemblies were irradiated differently. All but one of the PWRs was irradiated between 3 and 6 years, while the "typical" BWR assemblies remained in the reactor 1.4 years longer on average than "typical" PWR assemblies. The "typical" assemblies in this calculation did not include the 4 assemblies for which the initiation to discharge time was longer than 10 years.

Among the 25 PWR assemblies depicted on the left side of Figure 1, three assemblies stick out.

1. Assembly W was irradiated significantly less than would be expected; it was enriched to 3.6 wt.% but was only irradiated to 28.5 GWd/tU; an irradiation around 44 GWd/tU would be more typical of this initial enrichment.

2. Assembly O was irradiated more than was typical for its initial enrichment; it was enriched to 2.80 wt.% but was irradiated to 40.5 GWd/tU; an irradiation around 33 GWd/tU would be more typical of this initial enrichment.

3. Assembly X is atypical because it was irradiated for two cycles to about 19 GWd/tU, removed from

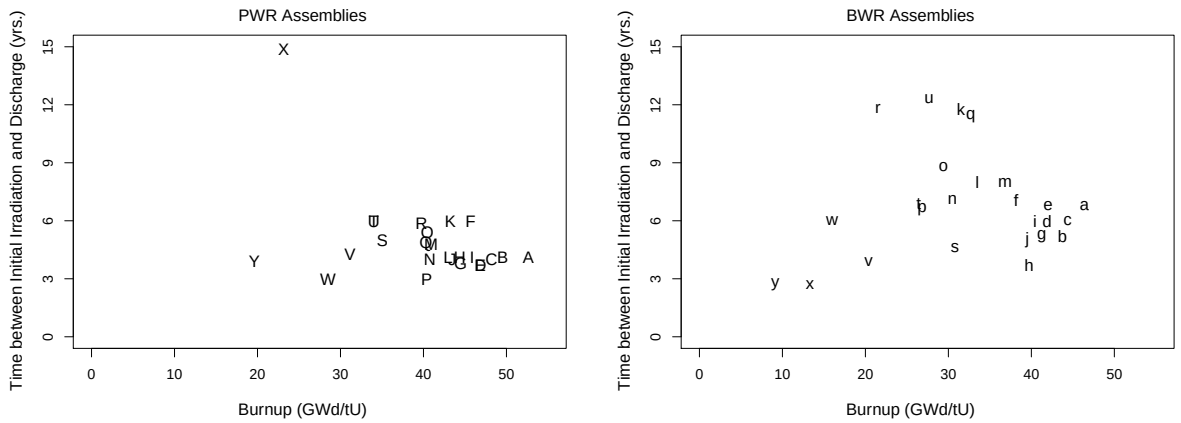

Figure 2: The time interval between the moment of initial irradiation and the final discharge is illustrated as a function of the burnup for the 25 PWR assemblies on the left and the 25 BWR assemblies on the right.

the reactor for about 10 years and then returned to the reactor for two more cycles during which it only liberated 4 GWd/tU more of energy. In Figure 2 it is clear how assembly X is different than all the other assemblies in terms of entry and exit from the reactor. It is interesting to note that Assembly X and Y entered a reactor within a day of each other and that they both produced about 19 GWd/tU of energy over 3 years. Then Assembly Y was permanently removed from the reactor and Assembly X sat out for 10 years before spending 2 more years in a reactor. Not much irradiation occurred during this later irradiation and, as a results, not many isotopes were produced, but the cooling time was delayed 12 years relative to Assembly Y.

Among the 25 BWR assemblies depicted on the right side of Figure 1, several assemblies stick out.

1. Assemblies t, v, w were irradiated significantly less than would be expected; assemblies x, y, r, u and l are a little less irradiated than typical; and Assembly "a" is a little more than typical.

2. Assemblies k, q, r, u were atypical because they remained in the reactor about 3 years longer than the other 21 BWR assemblies. This difference is not nearly as significant as was noted for the case with PWR Assembly X.

4 NDA Signal Integration Approach

Given that the Fork detector is the most commonly used integrated NDA instrument deployed by international safeguards organizations, the integration of the total neutron and gross gamma signals measured with the Fork is the base, or starting point, integration case. Considering the range of NDA instruments planned for deployment at Clab, the following seven integrations are currently planned: (1) Total neutron and gross gamma measured with a Fork detector, (2) Total neutron and isotopically specific peak area count rates measured from all four corners of an assembly, (3) Case two plus PNAR measured signatures, (4) Case two plus DDSI measured signatures, (5) Case two plus CIPN measured signatures, (6) Case two plus DDA measured signatures, (7) Case two plus heat plus any other NDA signatures.

It is likely that, as experience is gained, the selection of integrations cases, as well as the analysis approach, will evolve. The logic for the seven cases suggested above are the following:

- Case 1, the Fork detector, is a currently deployed instrument. The improvement obtained by using an Enhance Fork may be examined by including the spectral resolved passive gamma obtained from one corner of the assembly.
- Case 2 is a high quality measure of the total neutron and spectrally resolved passive gamma emission from all sides of the assembly. It is highly likely that this system or sub-system will be deployed at the encapsulation facility in Sweden; the inclusion of more advanced NDA instruments must improve upon Case 2 to justify their deployment. The total neutron measured for Case 2 is referred to as "high quality" because it will be made with the assembly centered inside of the detector with tight tolerances, approximately 5 mm on all sides; neutron detectors are on all sides of the assembly. With respect to the passive gamma signal, per simulation results, the sum of the measurements made from aligning a HPGe detector on each corner separately gives a representative average of the spectral line intensities from the three key isotopes of interest.
- Cases 3, 4, 5 and 6 each combine Case 2 with one additional neutron based NDA technique. These additional techniques contain some similarities. For example, they each can measure the multiplication of the assembly; the unique information provided by the individual techniques will become evident

through this integration effort. If beneficial effects are found to merit integration among these neutron techniques, additional cases may be studied. Note that gaining experience with the operational pros and cons among these techniques is an important safeguards achievement that will impact the future technology selection.

- Case 7 is singled out due to the uniqueness of measuring heat; the physics of this signature is clearly unique and inherently global. This is particularly of interest given the following speculations about a final deployment situation: (1) a calorimeter is likely to be in close proximity with other NDA equipment in an encapsulation facility in order to satisfy domestic heat calibration needs and (2) the long possible multiple hour measurement time needed with the calorimeter may not be a significant issue for the cases that might need extra attention such as extreme outliers. No suggestion is given for how heat may be integrated with the other instruments at this time; results presented in this report will inform such an integration.

5 Systematic Introduction of Declared Data

As described in the Introduction, the technical motivations for measuring spent fuel assemblies with NDA are driven by both safeguards and non-safeguards needs. With these different motivations may also come a difference in terms of what information can be included in the analysis. An international safeguards inspectorate such as the IAEA or Euratom may differ from the State regulator or SKB in terms of what declared information they are willing to trust. All parties would prefer an NDA analysis based solely on measured values but some parties may be willing to use some declared values if the ability to estimate useful parameters is significantly improved. Or some of the stake holders might be willing to use a declared value after the measured/estimated value is verified within a given tolerance. In light of this reality, a systematic approach with respect to the use of declared values in the analysis will be performed.

It is anticipated that the following scenarios will be analyzed with respect to the use of declared data: (1) no declared data, (2) initial enrichment only, (3) burnup only, (4) cooling time only. Depending on resources and interest, some analysis may be performed for which two of the three declared values just listed may be

taken as known quantities in the analysis. Given the time needed to perform all of these analysis scenarios, it is not clear at this time which NDA technique integrations will be involved in the full suite of scenarios outlined here. Most likely a subset of the outlined cases will be analyzed initially; then depending on the technical results and level of interests of relevant parties, more cases will be analyzed.

6 Scope and Approach of Analysis

The magnitude of the analysis proposed for this project is substantial. To summarize, there are 5 technical goals [missing pin detection, fuel characterization (initial enrichment, burnup and cooling time), Pu mass estimation, heat estimation, and reactivity estimation], 7 integrated NDA systems, and several scenarios in the context of declared data utilization. It is unlikely that the resources and/or technical motivation will merit the analysis of all cases; especially if PWR and BWRs require separate analysis. It is anticipated that lessons learned will enable the analysis to focus on a subset of cases, and that some conclusions can be generalized to the cases that may not be analyzed completely. Furthermore, research will be directed toward grouping as many assemblies as possible together by the use of "correction factors" as such groupings simplify the use of any research results for all interested parties. For the time being the fuel from PWR and BWR reactors will be analyzed separately given the understanding of how the isotopic evolution in these two reactor types are known to vary differently. After a separate analysis of both fuel types, it may become evident that a joint analysis is possible.

This report is anticipated to be a "living document" that will be updated as resources allows. This current report primarily focused on the characterization of the measured signatures relative to the quantities being predicted. The scope of the current analysis is determined by the data available. From a measured signature perspective, the following data, or input, is currently available:

1. **Spectral-resolved passive gamma** data obtained with HPGe detector.
2. **Total or gross gamma** data obtained with ion chambers of the Euratom Fork Detector.
3. **Total neutron** data obtained with fisson chambers of the Euratom Fork Detector.

In the course of this report some simulated results are analyzed. this was done so that the merit of the data could be explored and prepared for.

The end goal of this project is to estimate a variety of quantities of interest as discussed previously in this document. In the process of forming algorithms all significant uncertainties should be considered; yet, it is not always practical to do so. Below are some of the uncertainties of relevance to the quantities being estimated. They are listed here so as to not be forgotten in future analysis.

1. **Fuel characteristics (initial enrichment, burnup and cooling time):** It is noted that the values used for initial enrichment, burnup and cooling time were taken from SKB's DARK database, which is the "safeguards database." It is our understanding that the initial enrichment values in the DARK database are the "maximum average enrichment" and not necessarily the assembly average initial enrichment but rather in some cases they represent the initial enrichment of a subsection of the assembly. This is a point that may need further research if accurate initial enrichment estimation is considered a higher priority. At this point in the analysis, we want to note these subtle points.

2. **Pu mass** as calculated by SCALE[31]: Note we also have the Pu mass value calculated by the reactor operator using CASMO/Simulate/Polka[32]. Yet, because the operator-provided Pu mass is the Pu mass at discharge, a value that is not updated as a function of time, we made the decision to use the SCALE values calculated by ORNL estimated for the time of the NDA measurements.

3. **Multiplication** as calculated by MCNP[33]: For this current report the net multiplication is used as calculated for the central 90 cm axial length of the assembly when the assembly is in water inside the DDSI geometry with infinite reflecting boundaries used at the top and bottom of the model. Depending on the application of the information, the use of leakage vs net multiplication can be used. It is noteworthy that the DDSI detector, located approximately 9 cm from the fuel, has sheets of cadmium around the detector pods which suppresses the multiplication. This is not a concern for the analysis as the presence of the cadmium will have a systematic impact on the multiplication of all assemblies.

4. **Heat** as calculated by SCALE: Because only a few of the SKB-50 assemblies have been measured

with the SKB calorimeter, the heat values calculated with SCALE by ORNL, which include the heat generated by the fuel as well as the cladding and spacers, was used.

A theme of the integration or data mining analysis is to "allow the data to direct the research." What this means in practice is that a great deal of raw data is analyzed in this report. Once the raw data is processed and understood, models or some would say "corrections" will be made to the data; this is in contrast to many of the recently published work [8][11][13] for which much of the presented data was corrected for isotopic decay due to the known cooling time. Currently, the only information being taken as known for a given assembly is the assembly fuel type (17x17 PWR, 10x10 BWR, etc.).

7 Nuances among Initial Enrichment, Burnup and Cooling Time

Before discussing how the quantities to be predicted vary with measured signatures, it is important to state that the parameters of **initial enrichment, burnup and cooling time all influence the isotopic mix in any given assembly** that we will measure. For this reason an additional discussion of these three quantities is given here.

The **initial enrichment** is the weight percent of the ^{235}U isotope relative to the total amount of elemental uranium. The initial enrichment value is selected by the reactor operators when the assembly is purchased and indicates the amount of potential nuclear energy embodied in a given assembly "at birth." The initial enrichment can vary axially and radially within an assembly, particularly with BWR assemblies. In this report, as was stated earlier, the initial enrichment of an assembly is the "maximum average enrichment" provided by the DARK Database, which is the database containing the safeguards declaration data. The initial enrichment value in the DARK Database is not necessarily the assembly average initial enrichment but rather the initial enrichment of a subsection of the assembly. Putting together the facts that (1) the initial enrichment can vary axially and radially within an assembly and (2) the sensitivity of our neutron detectors also vary axially and radially over a small subsection of an assembly and (3) the initial enrichment is a property of an assembly that existed before the fuel entered the reactor and not a property of the assembly when we make our measurement, the task of nailing down the initial enrichment value is not a

simple task. We decided to use the value in the DARK Database as a general indicator of the initial potential energy given to each assembly foremost because this is the value that will be given to safeguards inspectors. In the future a researcher might decide to use the assembly average initial enrichment or customize each measurement to the average initial enrichment of the subsection of the assembly in the detector; these values are not currently available in our database.

The **burnup** is the amount of energy liberated from the assembly per unit mass of uranium (or heavy metal) often stated in terms of GW*days per ton of uranium. The burnup is determined with models that are coupled to heat measurements located at various locations within the core. The rate at which an assembly is "burned" or "burnt" in the commercial fuel context is determined by both the properties of the assembly at a given moment in time and by where the fuel is located in the core. As such, the rate of burnup can vary significantly in time through out the core.

The **cooling time** is simply how much time has passed since the reactor operator removed the assembly from the reactor for the final time. For typical fuel an assembly remains in the reactor for 3 to 7 consecutive cycles. In some cases the fuel may be pulled out of the reactor for an extended time interval between the first and last irradiation cycle. This fact renders some "cooling time corrections" inaccurate or biased as the time out of the reactor can be much longer than "typical" for some isotopes; hence, isotopes may decay significantly more than is corrected for when the declared cooling time is used. Or fuel may spend several years in the exterior of a reactor without significant irradiation induced change, yet all radioactive isotopes are decaying and the cooling time correction will not start until the fuel is removed.

8 Integration 1: Gross Gamma and Total Neutron - Fork Detector

8.1 Description of the "Raw" Data

8.1.1 PWR Assemblies

In the left side of Figure 3 the total neutron count rate is illustrated as a function of the gross gamma signal for the 25 PWR assemblies measured with the Euratom Fork detector. Color was used in this graph to indicate variation in cooling time. The dominant feature in this graph are the following: (1) Cooling time has an important impact on the evolution of the data in time. (2) For each of the 3 cooling time groups, an approximately linear relationship exists between the neutron and gamma signals; given the known formation mechanisms for the source terms for both gammas and neutrons, a linear relationship is not expected but within the limitations of the current data, such an approximate trend is as plausible as any other model. It is worth reminding the reader that two of the 25 assemblies depicted in Figure 3 are atypical: (a) Assembly X was in the reactor for 2 cycles, then remained out of the reactor for about 10 years, and then was returned to the reactor for 2 additional irradiation cycles. (b) Assembly W, compared to the other 24 assemblies, was significantly under-irradiated. Assembly W does deviate relative to the other assemblies of its cooling time group. We note that Assembly X is rather close to Assembly Y; we noted earlier that these two assemblies were very similar in all respects after 2 cycles but that Assembly Y was discharged at that time and Assembly X was irradiated 17% more, 10 years after Assembly Y was discharged. Assembly X is shifted relative to Y in a direction consistent with this scenario.

An additional point worth noting from the PWR data in Figure 3 is that the total neutron signal increased by a factor of 35 from the weakest to the strongest assembly, that is from assembly Y to A, while the gross gamma signal changed by only a factor of 6.0 between these same two assemblies.

8.1.2 BWR Assemblies

In the right side of Figure 3 the total neutron count rate is illustrated as a function of the gross gamma signal for the 25 BWR assemblies measured with the Fork detector. Color was used in this graph to indicate

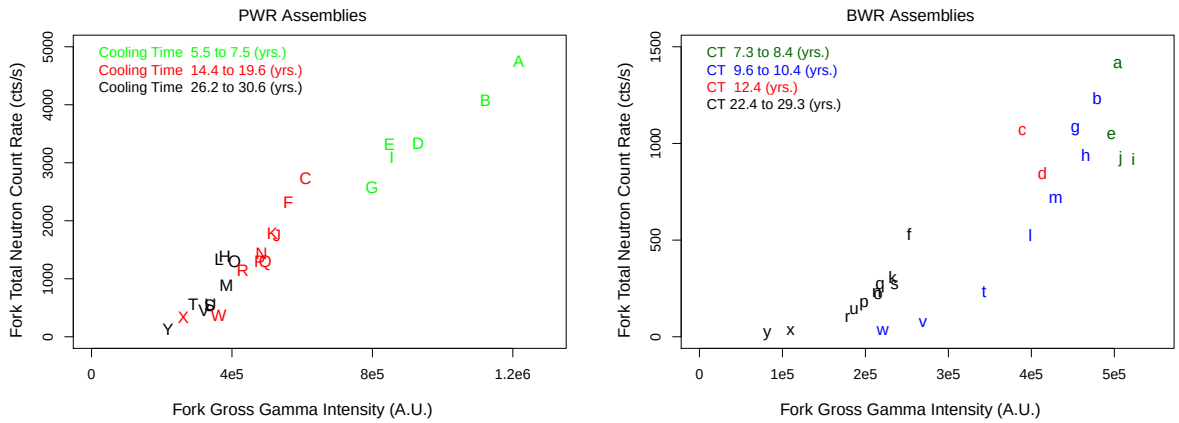

Figure 3: The correlation between the two predictors (total neutron and gross gamma) is illustrated for PWR and BWR assemblies. Color was used to group the assemblies into cooling time groups.

variation in cooling time. Additionally it should be noted that there is a difference in fuel type that correlated with cooling time with the black data points all being 8x8 assemblies and the non-black assemblies being 10x10 assemblies. There are 2 dominant feature from this graph: (1) For each of the 2 fuel types, the total neutron and the passive gamma signals smoothly correlate with each other; an indication of an exponential relationship is present, as would be expected given that the dominate gamma source term, ^{137}Cs, is expected to be produced linearly with burnup while the neutron source term is expected to scale as the third or fourth power of burnup. (2) There appears to be a cooling time functionality that impacts the correlation noted above in point (1) with assemblies that have cooled less emitting a greater gamma intensity. From research with the spectral resolved data published in [8] we know that a portion of the separation between the 8x8 and 10x10 assemblies is due to the assembly geometry such as pin diameter and pitch. A correction factor constant was calculated in [8] that enabled the 8x8 and 10x10 assemblies to be fit by one model.

An additional point worth noting from the BWR data in Figure 3 is that the total neutron signal increased by a factor of 141 from the weakest to the strongest assembly, that is from assembly y to a, while the gross gamma signal change by only a factor of 6.1 between these same two assemblies. Although the gamma intensity changes by essentially the same factor for the PWR and BWR assamblies, a factor of 6; the neutron intensity changed by a factor of 4 times more for the PWR assemblies. This is thought to be

primarily due to the elevated burnup of the PWRs, and secondarily, to the greater multiplication of the larger PWR assemblies.

8.2 Initial Enrichment, Burnup and Cooling Time Prediction

The purpose of this section is to illustrate how the assembly identification quantities, the initial enrichment, burnup and cooling time, that we want to predict vary with the measured signatures of a traditional Fork Detector. Along with the description of the data, well established trends in the gross gamma signature and total neutron count rate from past research, as well as the underlining basic physics, are described.

8.2.1 PWR Assemblies

Given that the detected gross gamma and total neutron signatures are influenced by the combined effect of the initial enrichment, burnup and cooling time, in addition to other properties of the fuel and reactor operation, it is challenging to discuss cause and effect. In order to illustrate the interrelated dependencies, the first three figures in this section are near identical depictions of the data. In all three cases the exact same gross gamma and total neutron data is illustrated as functions of initial enrichment, burnup and cooling time; the only difference among the three figures resides in the color of the data points. In Figure 4, color is used to group assemblies with similar initial enrichment; in Figure 5 the grouping is by burnup, while in Figure 6 the grouping is by cooling time. In all three figures, and throughout this report, each assembly was assigned the same unique letter of the alphabet to enable consistent identification, consistent with Table 1. Note that a small correction for cooling time was made for the assemblies count rates and intensities illustrated in this report to account for the fact that measurements were made throughout 2014. The count rates were adjusted to approximate the measurement of all assemblies on January 1, 2015. For this approximate correction the gamma intensity was taken to vary with the half-life of ^{137}Cs, which is 30.2 years; while the neutron emission was taken to vary with the half-life of ^{244}Cm, which is 18.1 years. No correction was made to account for the time that has passed since the fuel was discharged from the reactor.

The data in Figures 4, 5 and 6 were graphed in an atypical manner; what is generally considered as the

independent variable is usually graphed on the abscissa (x-axis) with the dependent variable on the ordinate (y-axis). The motivation for this decision was driven by the desire to consistently put the parameter to be predicted on the ordinate and the measured value used as input to the analysis on the abscissa.

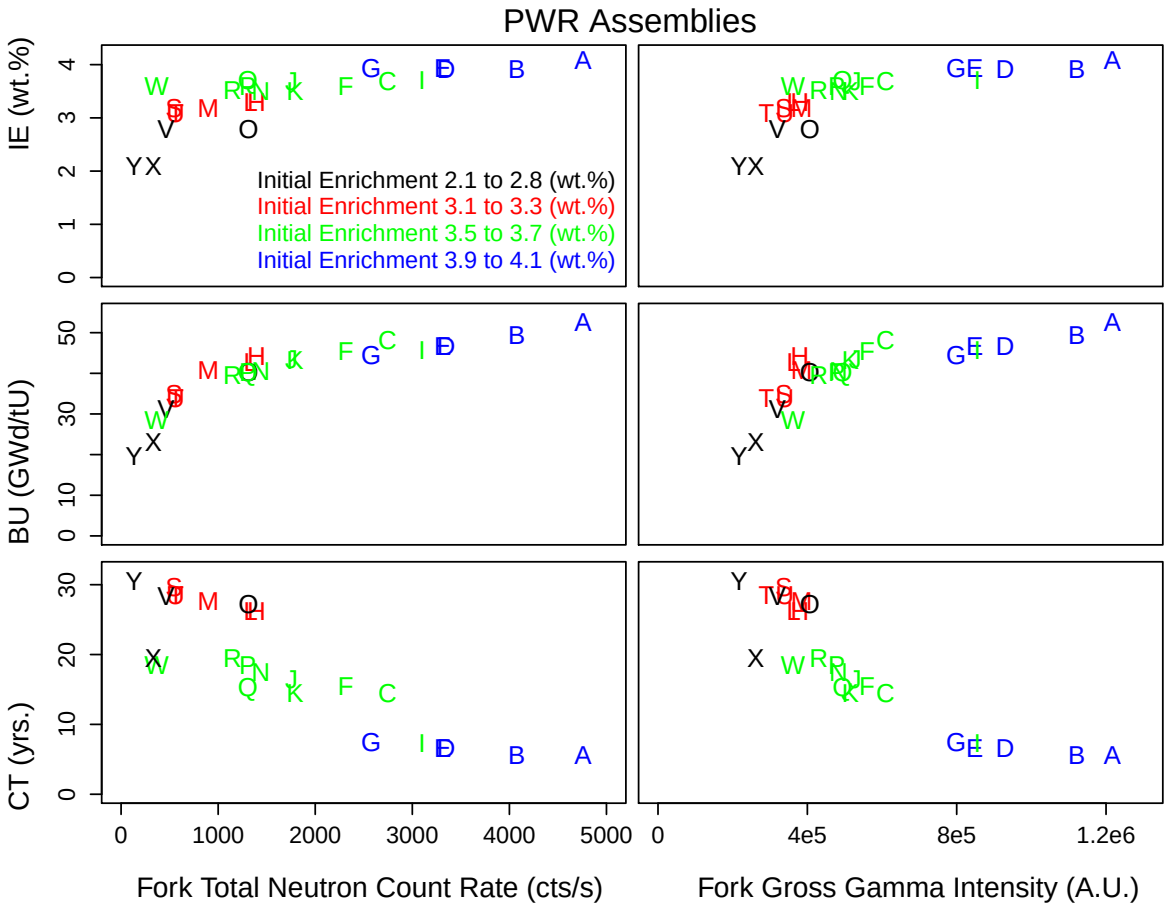

Figure 4: The correlation among the three quantities to be predicted, initial enrichment, burnup and cooling time, is illustrated as a function of the two measured predictors: total neutron count rate and gross gamma intensity. Color was used to divide the assemblies according to their initial enrichment as indicated in the ledger

In Figure 4 a few trends are evident. For the top two graphs, a rough correlation between initial enrichment and both the total neutron count rate and the gross gamma signal is observed. This is to be expected because, as the potential nuclear energy for thermal fission in an assembly is increased with

increased initial enrichment, the assembly is able to liberate more energy in the reactor and in the process produce more isotopes that emit gamma rays and neutrons. Assemblies W and O are noted as outliers, particularly with the total neutron count rate data, as was also noted in the PWR protion of the initial enrichment vs burnup curve of Figure 1. The degree of separation is more evident in the neutron signal than the gamma signal because neutron production is such a strong function of burnup and for most assemblies burnup and initial enrichment are correlated. Assembly X was previously noted as an outlier in Fugure 2 because it remained out of the reactor for a decade between initially entering the reactor and finally being discharged. Yet, Assembly X is not an outlier in the initial enrichment portion of Figure 4.

For the middle two graphs of Figure 4 the points depict less scatter evident with an apparent initial enrichment separation, particularly with the gamma data. The general trend of the total neutron emission correlating with the burnup raised to the third or fourth power is observed and is such a strong trend that it dominates over other factors [34]. The most dominant factor behind the observed correlation is the creation of ^{244}Cm, which has an 18 year half-life and is the dominant source term for neutrons particularly for the assemblies in the SKB-50. None of the assemblies appear as clear outliers.

For the bottom two graphs of Figure 4, the initial enrichment does not show any obvious structure with cooling time except for the fact that old assemblies were lower enriched so they were generally not irradiated as long and have been cooling for a longer time. Assembly X and Assembly I are outliers from the other assemblies that have similar initial enrichment values with both the neutron and gamma signals. Assembly W has a very small neutron count rate compared to the other assemblies in its initial enrichment group though the gamma intensity from Assembly W is not much removed from the other assemblies in its initial enrichment group. It is interesting to note that Assemblies X and Y which first entered a reactor within one day of each other produce nearly the same signal. If Assembly X were assigned the cooling time of Assembly Y, it would no longer be separated from the other assemblies of the same initial enrichment. As we comment earlier 83% of the isotopes in X and Y were produced at about the same time.

Because the data depicted in Figure 5 is only different from Figure 4 in that color in Figure 5 groups assemblies by burnup, the focus will be on interesting trends evident from the new grouping. In this context, all 6 graphs in Figure 5 are separated into high, medium and low burnup corresponding to high, medium

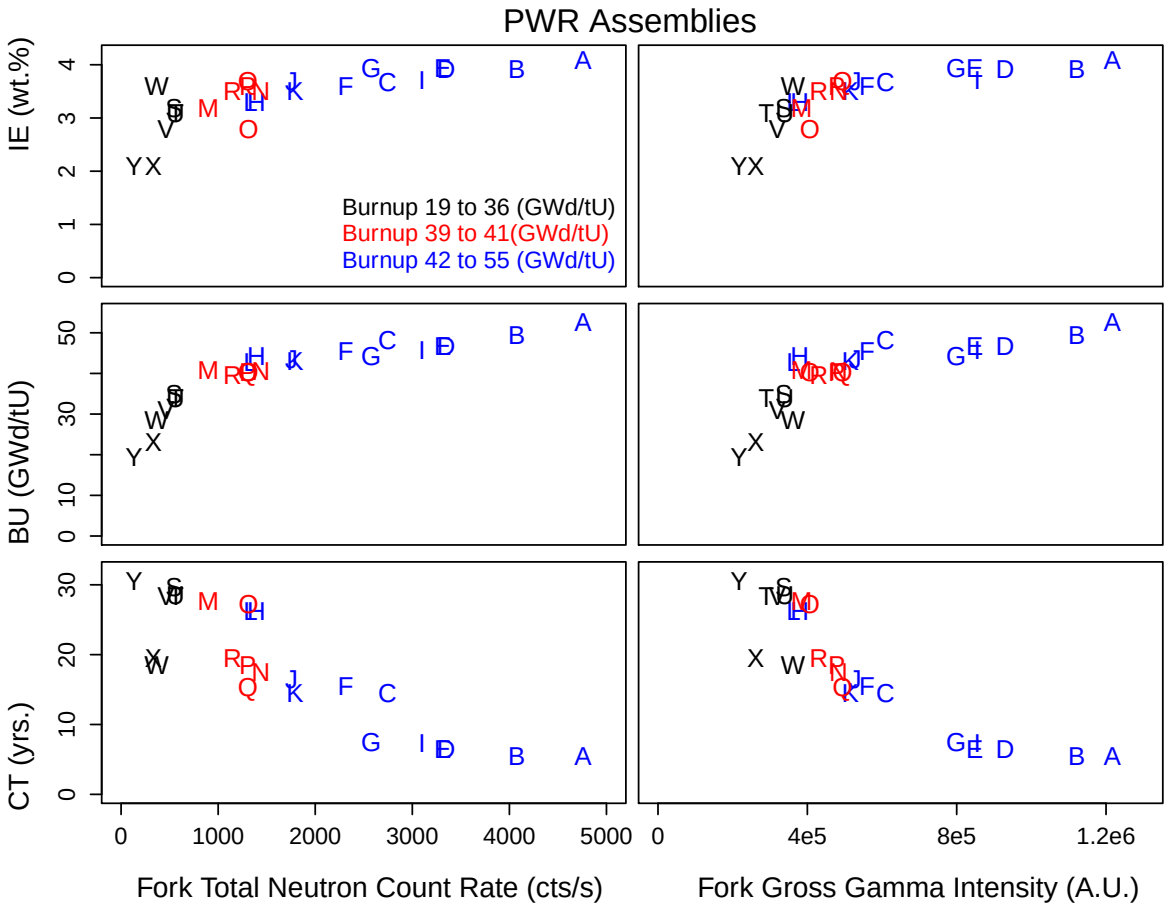

Figure 5: The correlation among the three quantities to be predicted (initial enrichment, burnup and cooling time) is illustrated as a function of the two measured predictors (gross gamma intensity and total neutron count rate). Color was used to divide the assemblies according to their burnup as indicated in the ledger.

and low signal intensity. Hence, although initial enrichment and cooling time definitely impact the signal, the burnup is the primary driver in signal intensity of the PWRs in the SKB-50 assemblies.

In Figure 6 color was used to emphasize three different cooling time ranges since the fuel was discharged from the reactor. The consistent correlation among the three cooling time groups is most evident in the middle burnup curve.

In Figure 7, the initial enrichment, burnup and cooling time are graphed as a function of the total neutron

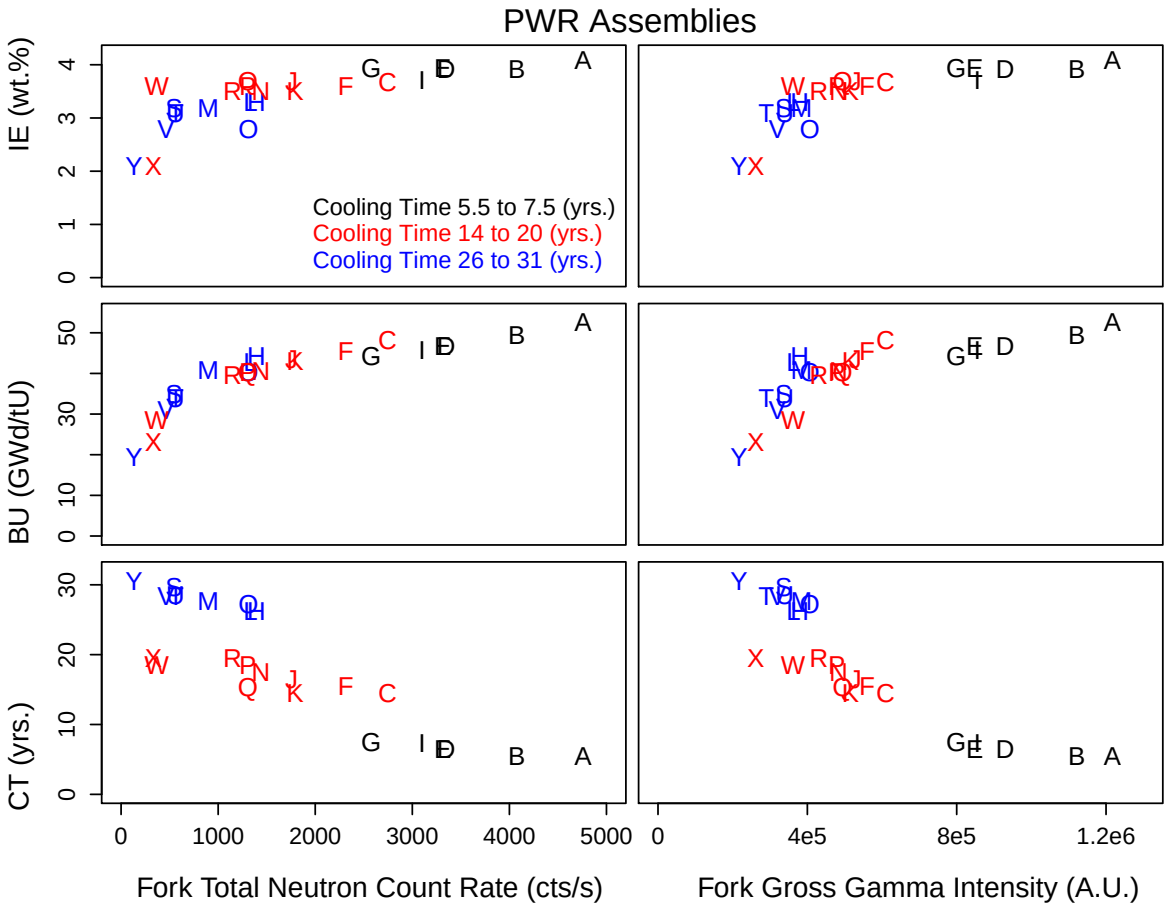

Figure 6: Correlation among initial enrichment, burnup and cooling time as a function of the total neutron count rate and the gross gamma intensity. Color was used to group the assemblies by cooling time with units of time in years.

count rate divided by the gross gamma intensity. The convention of coloring the data points by cooling time groups was followed on the left side of Figure 7 while for the right side the burnup grouping used earlier was applied. In the top two figures, where the ratio is graphed as a function of initial enrichment, the three assemblies (W and O, and possible X) noted as outliers in either Figures 1 and 2 are indeed outliers relative to the curve formed by the other 22 assemblies. In the middle, when the ratio is graphed as a function of burnup, the ratio of total neutron to gross gamma is a relatively smooth function with burnup **regardless of the cooling time.** Additionally, when the 25 assemblies are colored according to their burnup on the

right side of Figure 7, we see that the 25 assemblies generally fall into groups in each of the three graphs, indicating how burnup is a dominate factor in separating these assemblies.

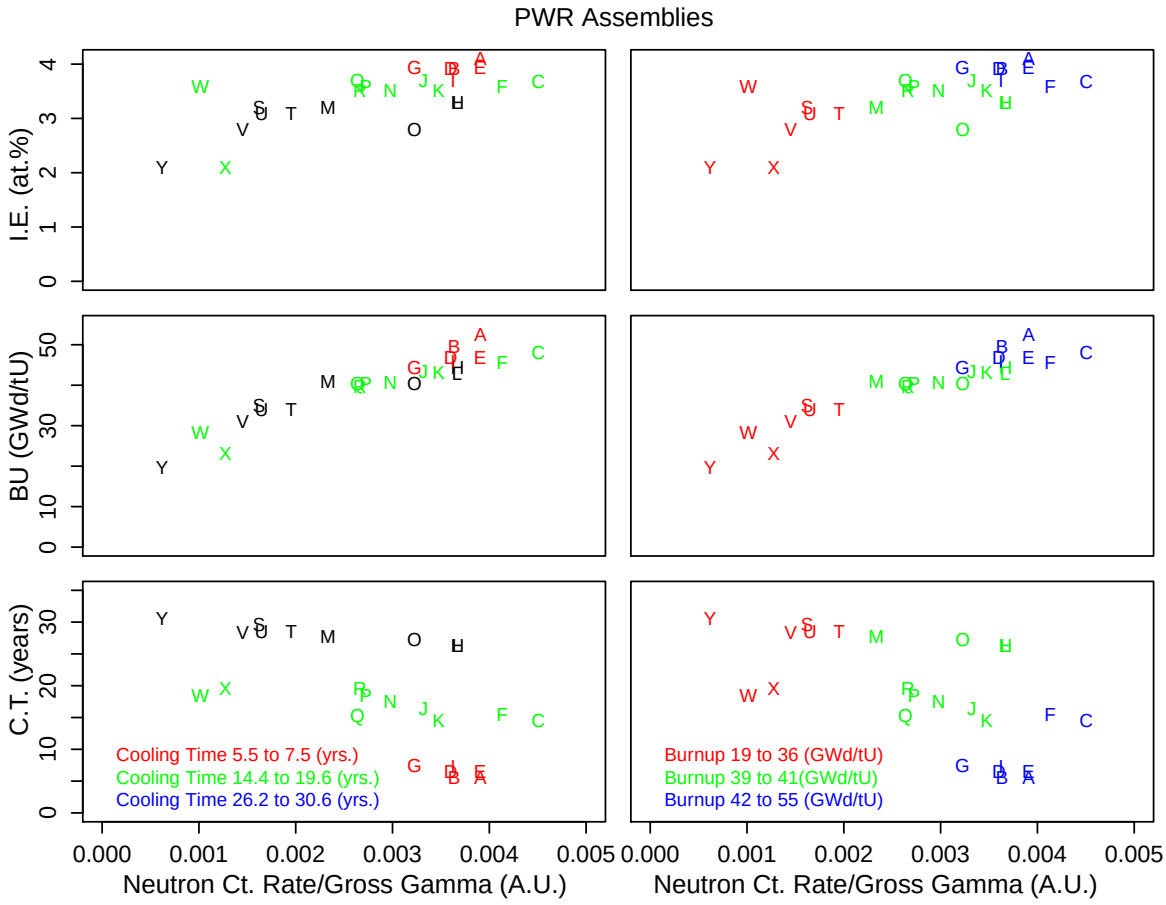

Figure 7: Correlation among initial enrichment, burnup and cooling time as a function of the quotient of the total neutron count rate divided by the gross gamma intensity. On the left side, color was used to group the assemblies by cooling time while on the right side color was used to group the assemblies by burnup levels.

8.2.2 BWR Assemblies

Because the BWR data follows the PWR data in this report, the BWR data will be discussed in comparison to the PWR data. The following are some of the main observations gleaned from the comparison among Figures 4, 5, 6, 7, 8, 9, 10 and 11:

1. The **initial enrichment vs. total neutron** count rate for both PWR and BWR assemblies are very similar in shape. In both cases the assemblies noted as outliers in terms of their burnup for their given initial enrichment in Figure 1 are also outliers in both the PWR and BWR cases. To accurately quantify what is an outlier requires statistics for a representative set of assemblies; as was noted earlier, many of assemblies in the SKB-50 were selected to span the diversity of fuel in Sweden and as such are anticipated to have as much if not more scatter than a random sampling of the same size; hence, outliers in this context are anticipated to be particularly outside the norm.

2. The **initial enrichment vs. gross gamma** intensity for both PWR and BWR assemblies are roughly similar. The assemblies noted as outliers in the total neutron count rate curve are not clearly outliers in the gross gamma data.

3. The **burnup vs. total neutron** count rate for both PWR and BWR assemblies is the smoothest relationship among all six graphs. As was noted for PWRs, the strong dependence of the neutron count rate dominates other dependences such as cooling time or initial enrichment. The general trend of the total neutron emission correlating with the burnup raised to the third or fourth power is observed and is such a strong trend that it dominates over other factors [34]. The most dominant factor behind the observed correlation is the creation of ^{244}Cm, which has an 18 year half-life and is the dominant source term for neutrons particularly for the assemblies in the SKB-50.

4. The **burnup vs. gross gamma** intensity appears rather different between the PWR and BWR assemblies. The separation into two groups is dominated by the 10x10 vs. 8x8 difference per [8]. Yet, once the outliers in terms of their burnup for their given initial enrichment in the right side of Figure 1 are ignored, a trend is observed that is clearly influenced by cooling time. The cooling time effect is

a combination of two primary factors: (a) ^{134}Cs contributes significantly for fuel cooled less than 20 years and (b) ^{137}Cs decays with a 30 year half life.

5. The **cooling time vs. total neutron** count rate and the **cooling time vs. gross gamma** intensity for both PWR and BWR assemblies has a very rough decreasing signal with cooling time when outliers, in terms of their burnup for their given initial enrichment, in Figures 1 are eliminated.

6. When the **initial enrichment, burnup and cooling time were graphed as functions of the ratio of the total neutron count rate to the gross gamma intensity**, the initial enrichment graphs were similar to those noted previously when the predicted quantities were graphed vs. neutron and gamma signatures separately. It is also noted that for both PWR and BWR assemblies the burnup correlated smoothly with the neutron to gamma ratio.

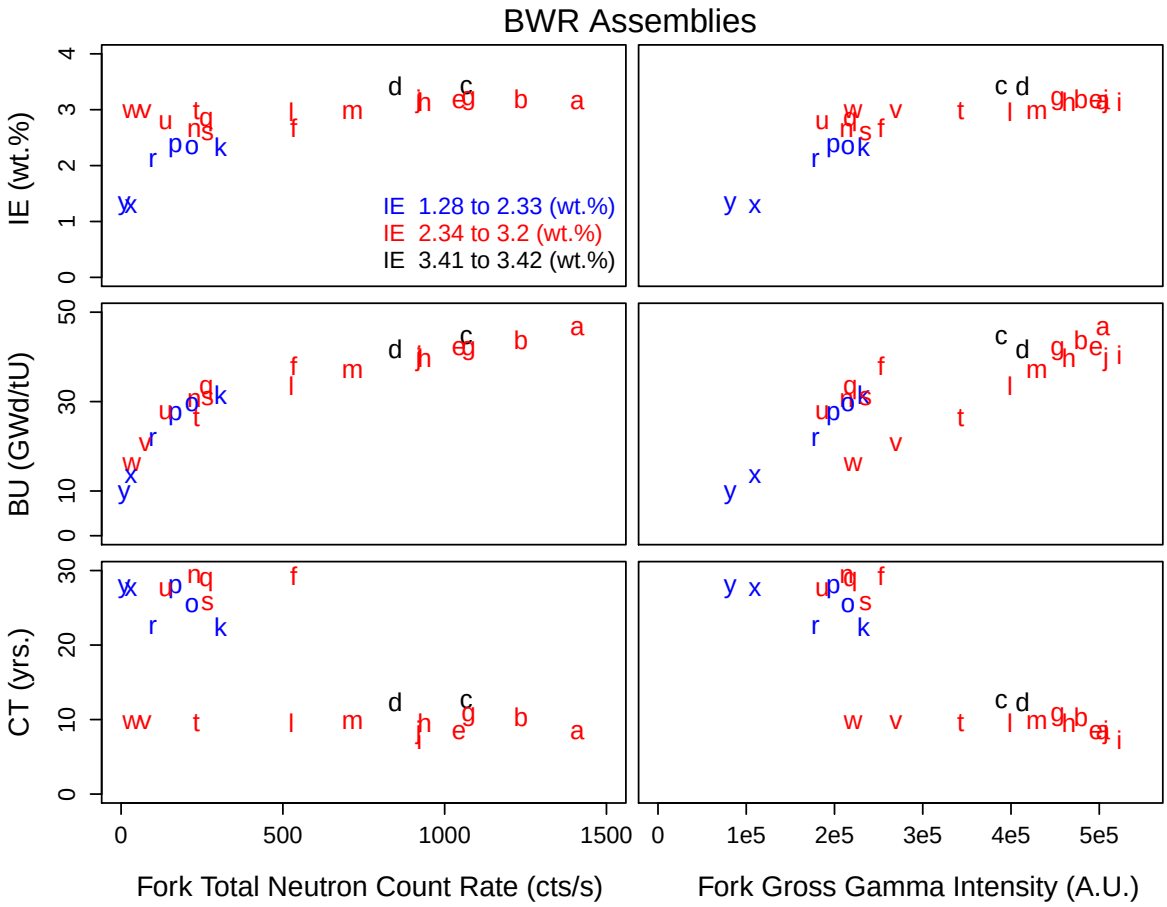

Figure 8: The correlation among the three quantities to be predicted, initial enrichment, burnup and cooling time, is illustrated as a function of the two measured predictors (total neutron count rate and gross gamma intensity). Color was used to divide the assemblies according to their initial enrichment as indicated in the ledger.

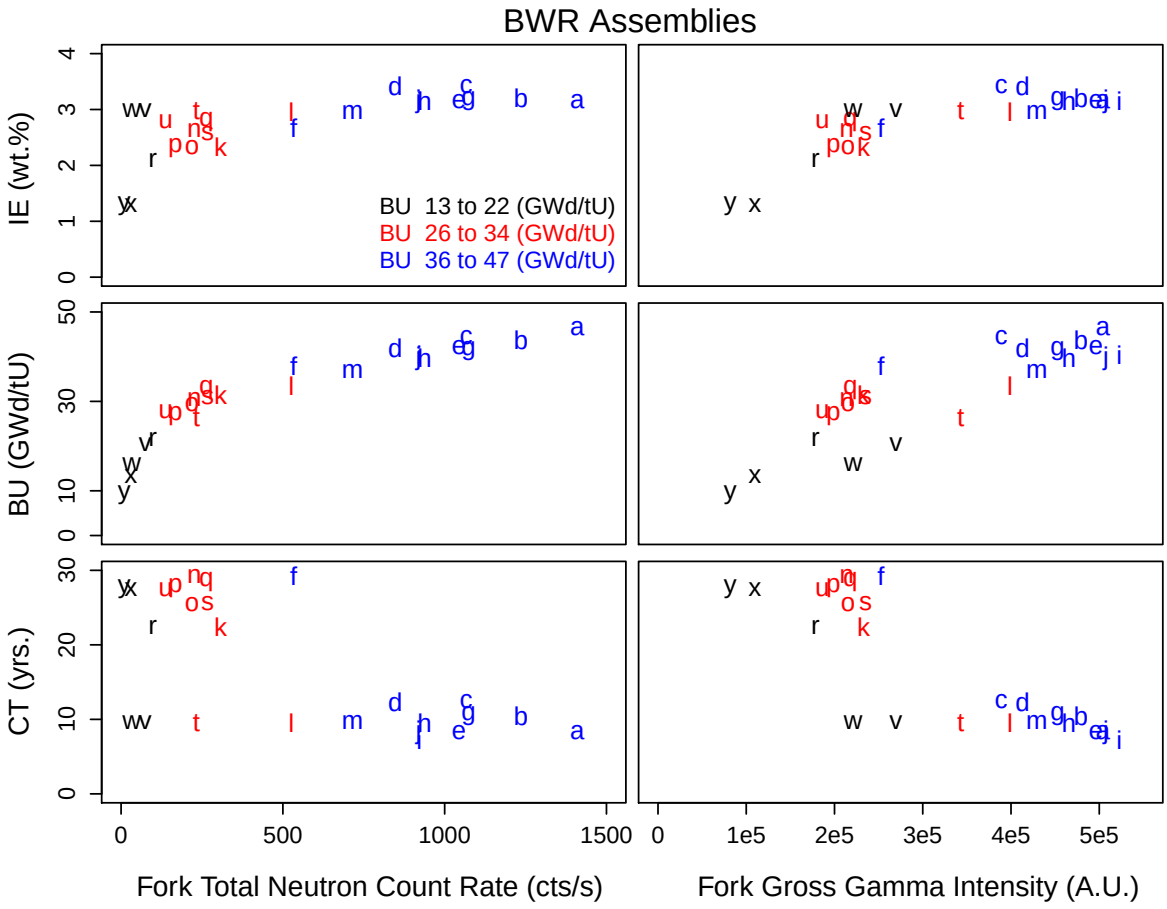

Figure 9: The correlation among the three quantities to be predicted (initial enrichment, burnup and cooling time) is illustrated as a function of the two measured predictors (gross gamma intensity and total neutron count rate). Color was used to divide the assemblies according to their burnup as indicated in the ledger.

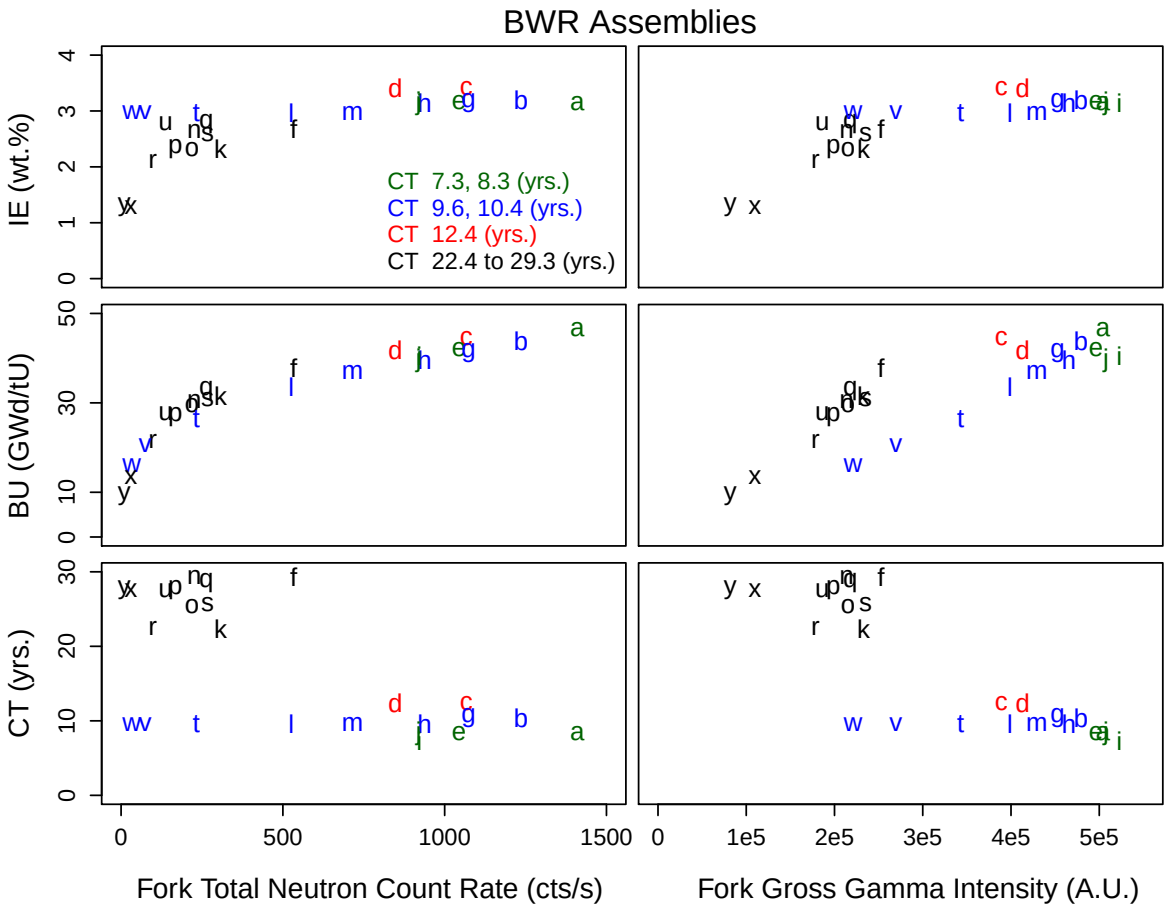

Figure 10: Correlation among initial enrichment, burnup and cooling time as a function of the total neutron count rate and the gross gamma intensity. Color was used to group the assemblies by cooling time with units of time in years.

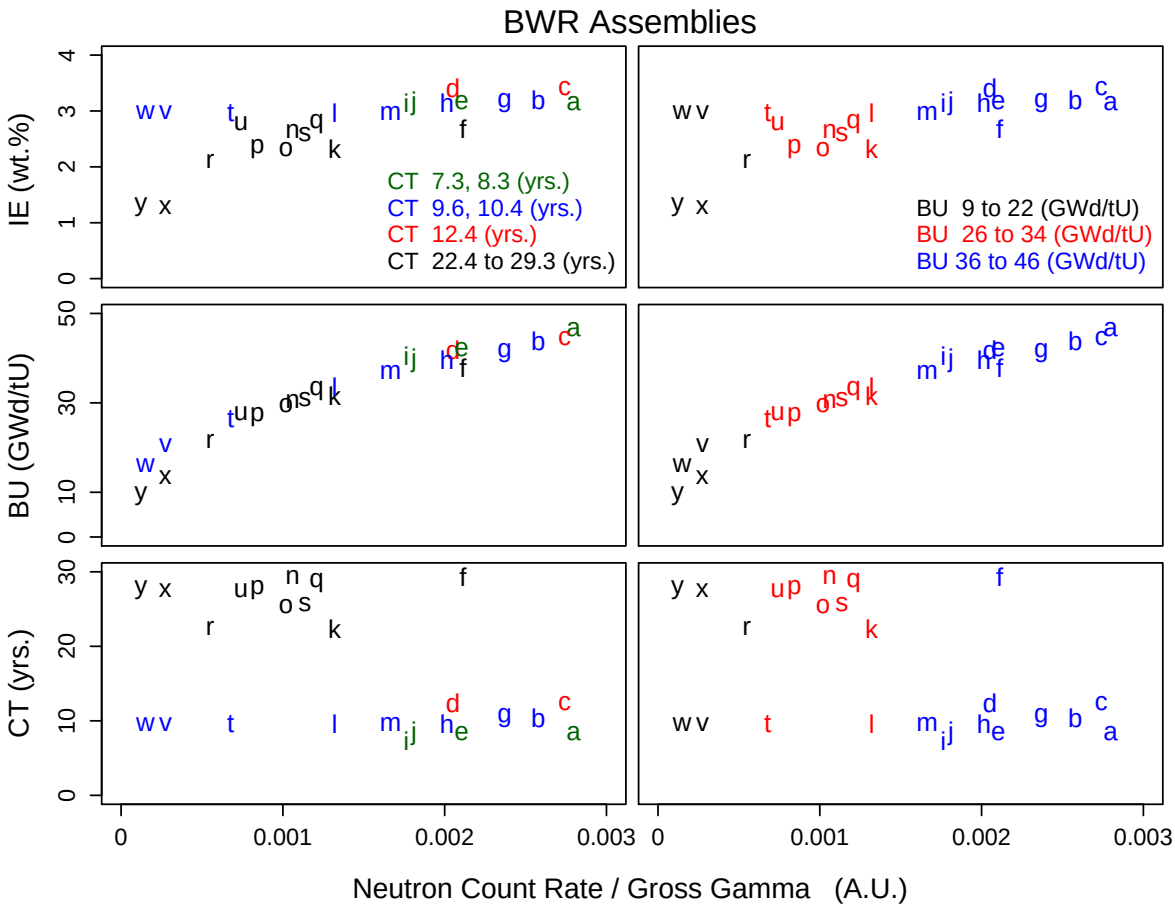

Figure 11: Correlation among initial enrichment, burnup and cooling time as a function of the ratio of the total neutron count rate divided by the gross gamma intensity. On the left side, color was used to group the assemblies by cooling time while on the right side color was used to group the assemblies by burnup levels.

9 Integration 2: Spectral Resolved Gamma and Total Neutron

In this section the utility of including spectral resolved gamma data is presented. Although the total neutron data will be integrated with the spectral resolved data in Integration 2, the primary focus in this section is on spectral resolved data as the total neutron signal was discussed in the previous section.

Given the expectation that only fuel in the 10 to 70 year time interval will be processed at the Swedish Encapsulation Facility (Clink), the discussion is focused on this time interval. Focusing on this time interval significantly focuses and simplifies the research as the gamma source term is much more complex in the discharge to 5 year time interval than it is after 5 years.

There are three primary isotopes in spent fuel emitting gamma rays likely to be useful in the 10 to 70 year time window of interest: ^{134}Cs, ^{154}Eu and ^{137}Cs with half-lives of 2.06, 8.6 and 30.2 years, respectively. For a gamma system optimized for the entire 10 to 70 year time, it is expected that the ^{134}Cs lines will only be detectable until the fuel is cooled approximately 20 years. A subtle point of this discussion is embedded in the phrase, "a gamma system optimized for the entire 10 to 70 year time interval." By this phrase it is anticipated that a spectral resolved detector setup will take advantage of the fact that ^{154}Eu emits gamma rays are significantly higher in energy than gammas from ^{137}Cs or ^{134}Cs; hence, attenuation placed between the detector and the fuel can render the gamma rays from ^{154}Eu incident upon the detector to be very strong relative to those from ^{137}Cs. It is also possible to optimize the system for the detection of ^{134}Cs; if one did so, one might extend the detection range by a decade to about 30 years.

For the encapsulation facility it is suggested that optimization is best guided by the detection of ^{154}Eu because gamma rays from this isotope can be detected for the full range of fuel entering an encapsulation facility as will be discussed later in this report. This point of optimal detector design is being discussed in this section for the following reasons: (1) The ability to detect lines from both ^{154}Eu and ^{137}Cs for all the cooling times of interest to Clink is the reason an emphasis is being given in the analysis to these isotopes. (2) Additionally, when data was collected at Clab, the count times were selected so that the sum of the data for all 4 viewing angles would have an uncertainty for the 1274 keV line of ^{154}Eu of 1% uncertainty or less. Note, the Clab spectral system is not optimized for the detection of the 1274 keV line.

Because it is fairly common to find publications that state that ^{154}Eu decays to undetectable levels [35] with the current roughly 50 year cooled fuel, a brief discussion of the fundamental physics and the context for the accuracy of this statement are given here. A 45 GWd/tU, 4wt.%, 5 year cooled assembly emits approximately 4 x 10^{13} 1274 keV photons/s [7]. When this assembly is cooled to 70 years it emits approximately 2 x 10^{11} 1274 keV photons/s or 5 x 10^{8} 1274 keV photons/s per centimeter of axial length. Given that more than 20% of 1274 keV photons are expected to escape a 17x17 assembly unattenuated, that leaves approximately **1 x 10^{8} 1274 keV photons/s per centimeter of axial length** available for detection by a plausible detection system located around the assembly. Of note, this same assembly at 70 years is expected to emit 6 x 10^{11} 662 keV photons/s per centimeter of axial length or **6 x 10^{10} 662 keV photons/s per centimeter of axial length** if we assume only 10% of these lower energy photons escape the assembly unattenuated. So the bottom line is that **there are plenty of detectable photons in this 70 year old assembly from both ^{154}Eu and ^{137}Cs** and because the production of ^{154}Eu and ^{137}Cs is very roughly linear with burnup, one can be confident that lower burnup fuels will also have plenty of photons available to detect from both isotopes even when the fuel is 70 years cooled.

Given that most higher count rate, off-the-shelf, detection systems are limited to detecting on the order of 10^{6} photons/s the key issue is how the detector system can be designed to manage the fact that we have more photons available than our detector system can handle. The detector designer has three primary choices for managing the large count rate: (1) distance, (2) collimation and (3) attenuation. Because most detector systems are designed to detect localized information from a broad diversity of isotopes in the fuel, distance and collimation are the primary means selected to lower the count rate. Yet, for the case of spent fuel measurement in the 10 to 70 year cooling time window, using attenuation allow the detection system designer to detect gammas from both ^{154}Eu and ^{137}Cs for well over 70 years after discharge. In the comparison above, the 662 keV line was 600 times stronger after 70 years of cooling, as compared to the 1274 keV line; yet, 10 cm of lead attenuated the 662 keV photons 467 times more effectively than the 1274 keV line of ^{154}Eu. **Including this 10 cm of lead means the un-collided photon intensity emitted around all sides of the assembly from a 1 cm vertical extend of fuel is on the order of 1 x 10^{5} photons/s independently for both the 662 and 1274 keV spectral lines.** Hence, a system for detecting both lines can be designed. The reason researchers frequently conclude otherwise, it is speculated,

is because they extrapolate the detection limit for systems that used primarily distance and collimation for count rate management.

9.1 Description of the "Raw" Data

In Figure 12 the ^{137}Cs intensity as a function of the burnup is graphed. Two very common trends are noted: (1) the intensity of the ^{137}Cs peak for a given cooling time group is a near linear function of burnup. And (2) there is a cooling time dependence evident among the three arbitrarily selected cooling time groups. If you look carefully within cooling time groups further cooling time dependence is evident. Given the more complex and variable irradiation experience with BWR assemblies, there is more scatter among the BWR assemblies.

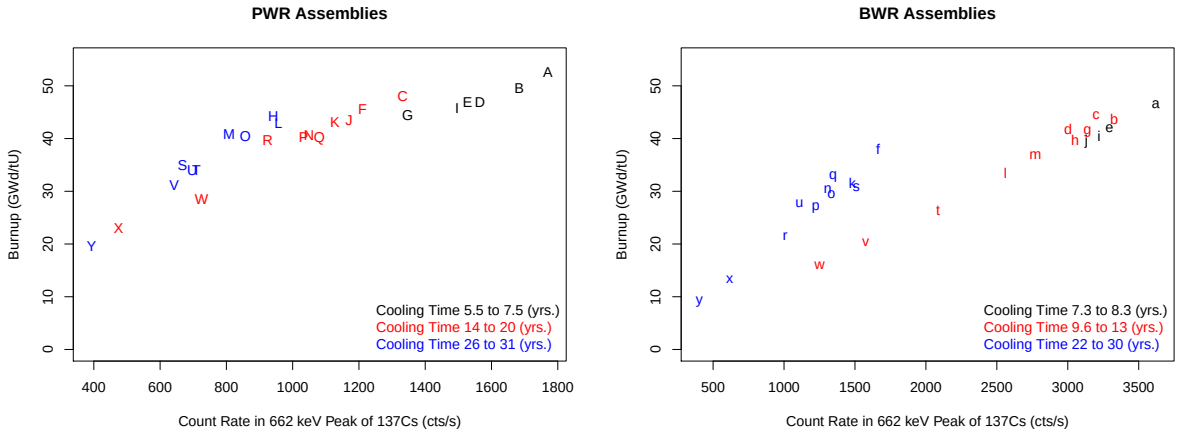

Figure 12: Burnup as a function of the 662 keV peak of ^{137}Cs is illustrated in separate graphs for the PWRs and BWRs of the SKB-50 assemblies.

In Figure 13 a nearly linear relationship is noted between the ^{154}Eu intensity and burnup as well. It is worth noting that the assemblies that produce the most scatter are often the extremes of a cooling group. For example Assemblies R and P are the longest cooled assemblies among the red colored PWR assemblies, this is particularly important given that the half-life of ^{154}Eu is 8.6 years and the red cooling time grouping encompasses 7 years. Similarly among the BWR assemblies, Assemblies c and d are two of the oldest while Assembly k is the least cooled in its cooling time grouping. Yet, as noted with the ^{137}Cs intensity, more

scatter is evident among the BWRs relative to the PWRs.

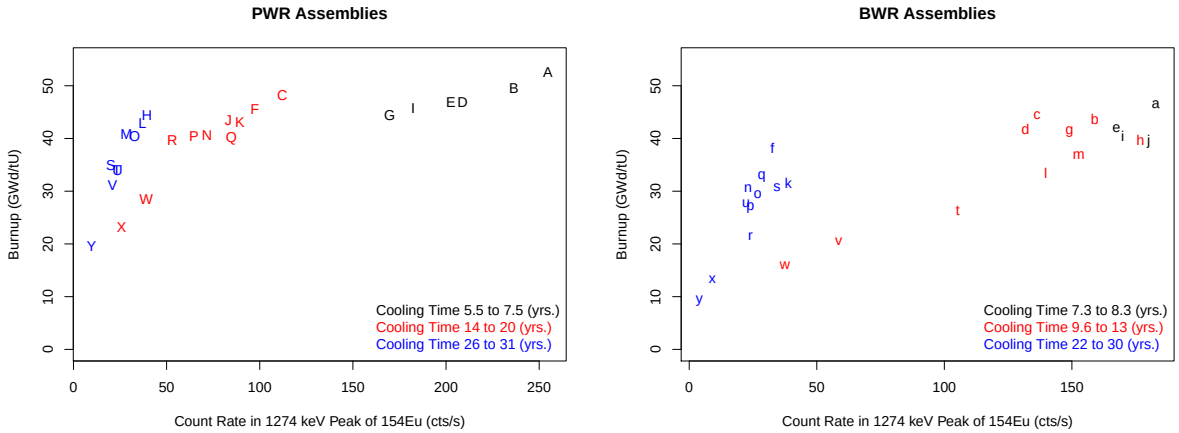

Figure 13: Burnup as a function of the 1274 keV peak of ^{154}Eu is illustrated in separate graphs for the PWRs and BWRs of the SKB-50 assemblies.

Given the complicated production mechanisms that produce ^{154}Eu, a process that involves approximately 20 different production chains[36] and a process that is known to be nonlinear as a function of burnup[35], the observed approximate linearity with burnup might be construed as surprising. Yet, it is suggested that as each assembly is irradiated, though the amount of ^{154}Eu that is produced is not linear per unit burnup, the end result of irradiation produces a nearly linear relationship because most all assemblies go through the same "fission evolution." The intended meaning of "fission evolution" is that each assembly starts irradiation by primarily fissioning ^{235}U while before final discharge most assemblies generate energy by fissioning primarily ^{239}Pu. We know that significantly more ^{154}Eu, is produced per unit burnup late in an irradiation cycle as compared to at the beginning because the fission of ^{235}U produces significantly less ^{154}Eu than does the fission of ^{239}Pu.

In Figure 14 the detected signal from ^{134}Cs is illustrated. Although our analysis does not focus on this isotope it is included to give a taste of some of the data. Furthermore it may be of use in the 10 to 20 year time frame during which it is easily detected. Note in Figure 14 the strong cooling time dependence. Relative to the 2.1 year half-life of ^{134}Cs the arbitrarily selected cooling time groups are very large and as such significant scatter is noted within cooling time groups. In future analysis when a cooling time correction

is applied to the data, additional insight will be gained.

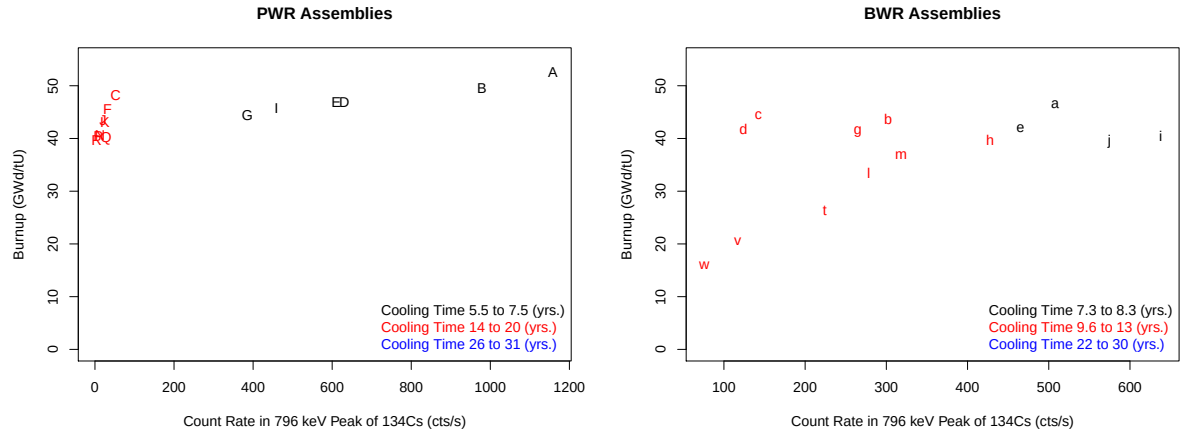

Figure 14: Burnup as a function of the 796 keV peak of ^{134}Cs is illustrated in separate graphs for the PWRs and BWRs of the SKB-50 assemblies.

In Figures 15 and 16 the ratio of the 1274 keV line of ^{154}Eu to the 662 keV line of ^{137}Cs is graphed as a function of burnup and cooling time, respectively. The most interesting graph among these is the smooth relationship between this gamma ratio and cooling time for the PWR assemblies in Figures 16. As with essentially all the dependencies, the scatter is greater among the BWR assemblies. For the BWR assemblies there are three significant outliers, all of which have been noted previously: Assemblies w and v which were significantly under irradiated and Assemblies x and y which were starter assemblies of very low initial enrichment (1.27 wt.%). It is surprising in the PWR side of Figure 16 that Assembly X is not as large of an outlier as one might expect. It is thought that Assembly X, by chance, sat out of the assembly long enough and then reentered long enough to obtain nearly the same ^{154}Eu and ^{137}Cs ratio as an assembly that underwent a typical irradiation. In Figure 15 a subtle trend is noted; within each cooling time group, the older assemblies were irradiated less than the more recently discharged assemblies.

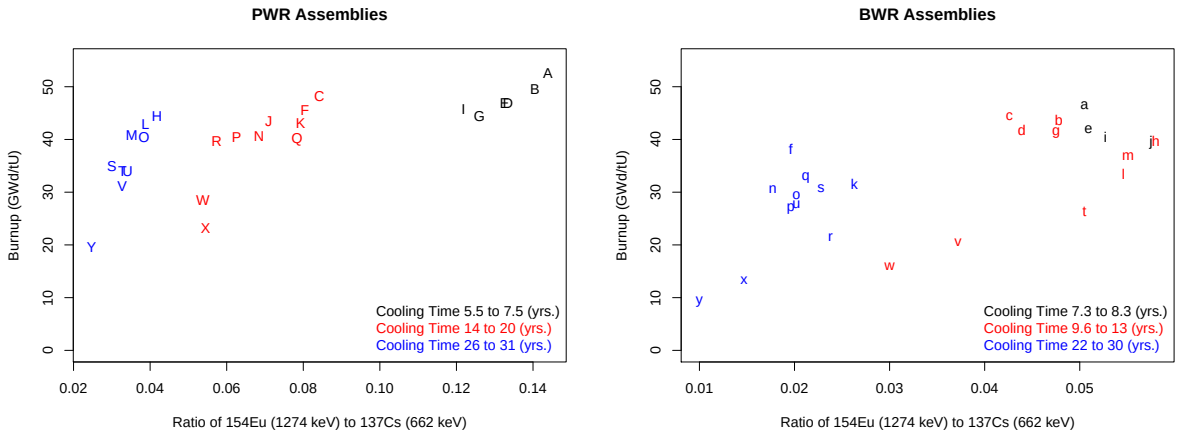

Figure 15: Burnup as a function of the ratio of the 662 keV peak of ^{137}Cs to the 1274 keV peak of ^{154}Eu is illustrated in separate graphs for the PWRs and BWRs of the SKB-50 assemblies.

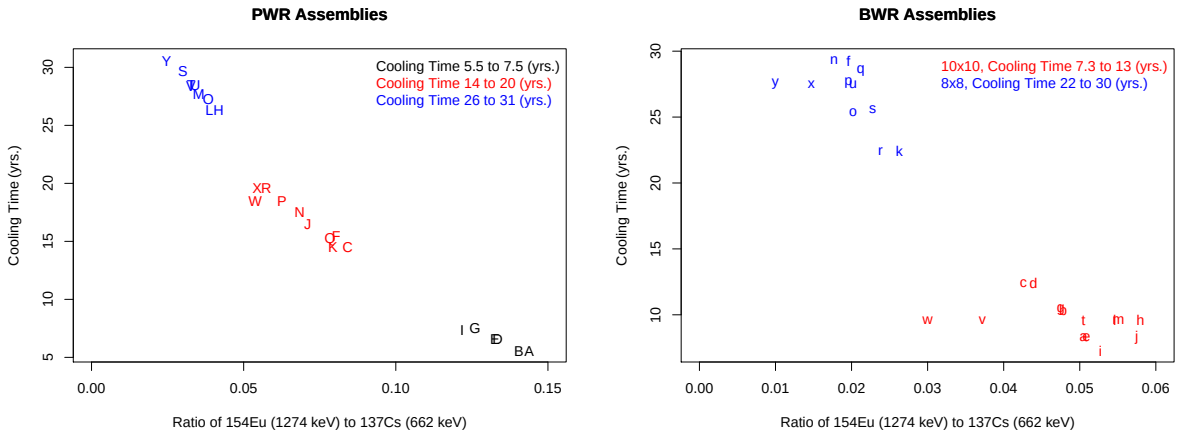

Figure 16: Cooling time as a function of the ratio of the 662 keV peak of ^{137}Cs to the 1274 keV peak of ^{154}Eu is illustrated in separate graphs for the PWRs and BWRs of the SKB-50 assemblies.

10 Integration 3 to 6: Spectral Resolved Gamma, Total Neutron and Multiplication

In 2017 and 2018 we anticipate the deployment of two NDA instruments that will allow the examination of the experimental capability of two passive NDA techniques (PNAR and DDSI) and two active NDA techniques (DDA and CIPN [or more accurately NGIPN because a neutron generator will be used instead of a Cf source]). It is worth emphasizing that the resources involved in going from one passive and one active NDA deployment to two passive and two active represents a small increase in hardware cost and deployment cost. The motivation for testing all four is to examine both the unique technical capability of each technique along with practical deployment issues.

10.1 Discussion of Multiplication in the Context of this Research Effort and Safeguards in General

Multiplication was initially listed as a technical goal in this project due to our collaboration with SKB because SKB needed to assure that all possible future spent fuel configurations, particularly those involving the spent fuel containers to be used in the repository, are safe from a criticality perspective. This was an easy research goal to add as several of our instruments measure multiplication; up to this time Pu mass quantification had been the main driver for measuring multiplication. Yet, as our research has advanced, important additional motivations for measuring multiplication have arisen:

1. As discussed previously, initial enrichment, burnup and cooling time all impact the isotopic content of the fuel. As our task is to measure the signatures emitted by those isotopes and then infer from the signatures various properties of the fuel, understanding the relationship among initial enrichment, burnup and cooling time is crucial. **Multiplication is highly valuable in this context as it can quantify the degree to which the potential nuclear energy of a given assembly, by virtue of its initial enrichment, was consumed through irradiation.**

   The underlying data analysis philosophy of **pattern seeking** that we are applying is driven by the

reality that (1) all LEU spent fuel starts out as a relatively simple isotopic entity, primarily comprised of three isotopes ^{235}U, ^{238}U and ^{16}O. (2) In the typically 3 to 8 years that the fuel spends in a reactor, the isotopes evolve in a process driven by the reactor operators desire to optimally extract energy from that assembly. (3) After leaving the reactor the isotopes in the fuel change in a very predictable manner, with unstable isotopes decaying in accordance with their known half-lives. The reason for discussing this three phase evolution in the context of multiplication is to highlight the role that multiplication plays in measuring where a given fuel assembly is in the evolution. Hence, multiplication is an indicator of whether or not the isotopic evolution of the fuel was carried to typical fruition or if the fuel was under irradiated or over irradiated and by how much.

2. Multiplication may merit being a safeguards metric, in and of its own right, a suggestion that is described in the section below on "Why Multiplication May be of Interest to Safeguards." Ideally, NDA instruments would exist that could easily measure the Pu mass in an entire assembly in water and as such enable mass accountancy; unfortunately, there is no such technology. Given this absence, a multiplication measurement can enhance the current item accountancy approach currently applied in international safeguards provided the measurements are fast, low cost and robust.

3. The measurement of multiplication is a much better manner of addressing the criticality concerns of spent fuel management personnel than the current gamma-based burnup credit measurements made by industry. The key issue is that the key people in industry are unaware that fast, low cost and robust hardware exists for multiplication measurement. Safeguards would benefit by industrial application of multiplication hardware.

10.1.1 Definition of Multiplication

Per the Passive Nondestructive Assay of Nuclear Materials [34] book, the definition of multiplication, M, is "the total number of neutrons that exist in the sample divided by the number of neutrons that were started. If 100 neutrons are started in the sample and an additional 59 are found to be created from multiplication events, the multiplication is 1.59." The multiplication is related to the "multiplication factor," k_{eff}, by the equation $M = 1/(1\text{-}k_{eff})$; for the example just described, k_{eff} is 0.37. The definition of k_{eff} is the "ratio of

the number of neutrons produced in one generation to the number of neutrons either absorbed or leaked in the preceding generation."[34]

10.1.2 Why Multiplication May be of Interest to Safeguards

The measurement of an individual assembly's multiplication can improve the quality of spent fuel safeguards for the following reasons: (1) Multiplication indicates that fissile material, **the material of primary proliferation concern**, is present. This compliments techniques such as tomography that measure the emission of fission products only. (2) Neutron multiplication penetrates the entire assembly and can be measured for all commercial fuel of interest to an encapsulation facility. Insertion of an isotopic point source is a typical diversion scenario, which could trick a total neutron count rate analysis, yet an isotopic source would not increase the multiplication. (3) In contrast to the other measurable spent fuel parameters, such as total neutron and passive gamma, the multiplication is nearly a constant quantity for typically irradiated spent fuel of a given fuel type as illustrated in Figure 17. Furthermore, for those few atypically irradiated assemblies, multiplication can quantify the degree to which a given assembly was under or over irradiated, a property which can be checked with the declaration. (4) Unlike radiation from ^{134}Cs, ^{137}Cs, ^{154}Eu or the passive neutron count rate, the multiplication value of an assembly is generally not significantly impacted by large breaks in reactor operating cycles. This is due to the strong economic motivation of reactor operators to optimally irradiate each assembly; the reactor operators know the history of the fuel best, and if operating a reactor for peaceful purposes, will optimally extract energy from each assembly.

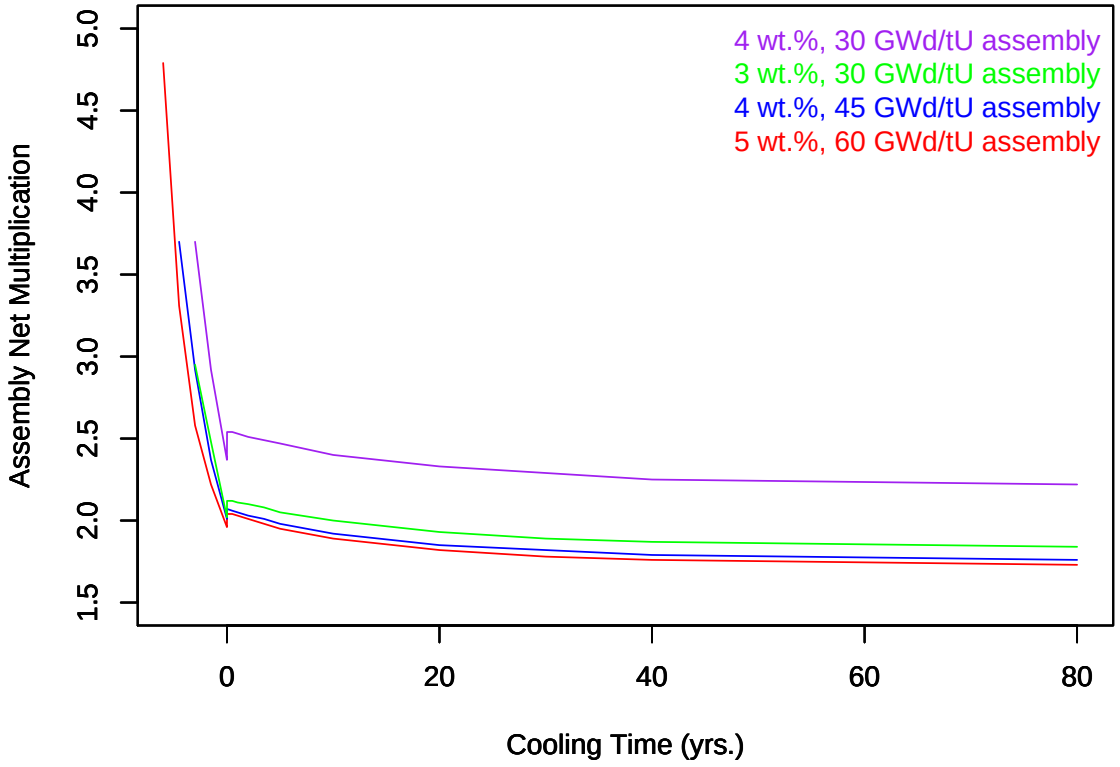

Figure 17: The multiplication of three approximately fully burnt assemblies is illustrated as a function of time and one partially irradiated assembly (4 wt.%, 30 GWd/tU). The time t=0 represent when the assembly was discharged from the reactor. The maximum multiplication for each assembly indicates its pre-irradiation multiplication, when the assembly was fresh.

Most of the signatures measured from a spent fuel assembly; such as ^{134}Cs, ^{137}Cs, ^{154}Eu or the neutron count rate; change by multiple half-lives between discharge and 80 years. In contrast the multiplication is expected to change by only about 15% over this same time interval. This constancy among the change in other signatures provides an appealing property for an integrated NDA system. Most specifically to the spent fuel acceptance criteria of the Swedish repository of 10 to 70 years cooling time, the multiplication is only expected to change by about 7% over this time interval.

10.2 Description of the "Raw" Data in Context of Multiplication

10.2.1 PWR Assemblies

The simulated results for the SKB-50 assemblies depicted in Figure 18 provide context for the discussion of the utility of measuring multiplication to indicate degrees of irradiation. Previously we noted that PWR Assemblies W and O and BWR Assemblies w, v and t were outliers in the initial enrichment vs. burnup graph of Figure 1.

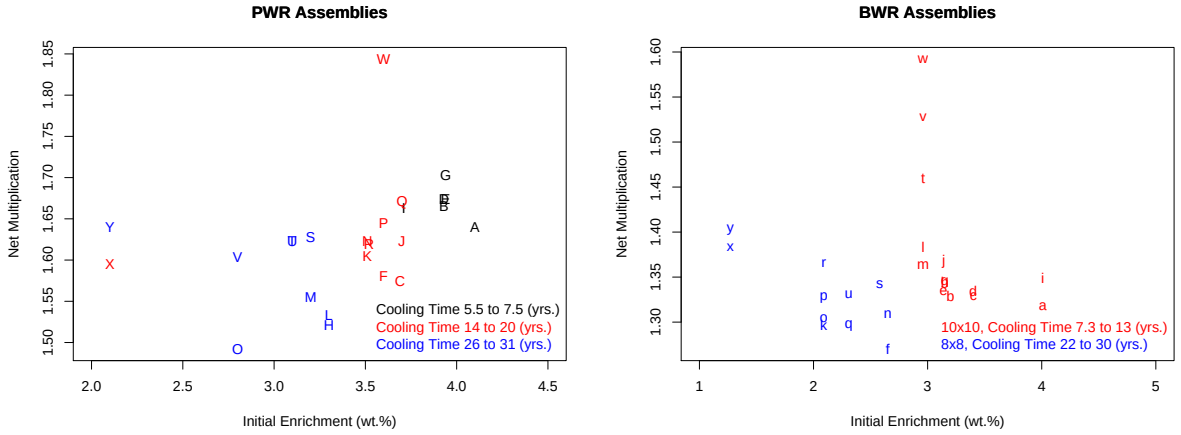

Figure 18: The simulated net multiplication of the PWR (left) and BWR (right) assemblies when situated inside the DDSI instrument is illustrated as a function of the initial enrichment.

In Figure 18 we see that W has the highest multiplication among the PWR assemblies while O has the lowest; furthermore, among the BWR assemblies w, v, and t are very clear outliers. Following the deployment

of the 4 neutron techniques we will have a good idea of the magnitude of the **systematic uncertainty of each technique relative to the expected multiplication differences** among the assemblies.

A trend among the three cooling times groups is evident in Figure 18, particularly when the outlier assemblies W and O are excluded. The average multiplication of each group decreases from 1.67 for the 5.5 to 7.5 cooling time group, to 1.62 for the 14 to 20 year group and then to 1.59 for the 26 to 31 year group. The total change in multiplication from the shortest cooling time group to the longest cooling time group is 12% recalling that 1.0 represents the bottom of the multiplication scale; this change is consistent with the change depicted in Figure 17. Among the BWR assemblies there is also a decrease in the multiplication from the youngest fuel to the oldest but there is the added complication that the fuel structure changed significantly between the 8x8 and 10x10 assemblies; the change from 15x15 to 17x17 did not seem to have a large impact on multiplication.

In Figure 19 there is structure within each cooling time group; the multiplication generally decreases as the burnup increases; this pattern is particularly noted when the outlier assemblies W, O are excluded and if you think of the "starter core" assemblies X and Y as outliers as well. It is expected that such structure would have its root cause in reactor operation. Why this particular trend exists is not known at this time.

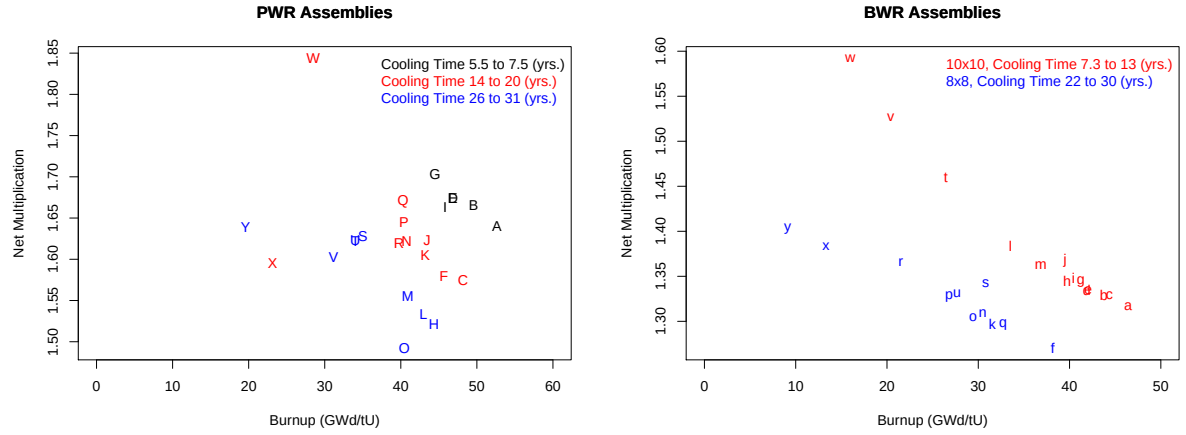

Figure 19: The simulated net multiplication of the PWR (left) and BWR (right) assemblies when situated inside the DDSI instrument is illustrated as a function of the declared burnup.

For the PWR assemblies in Figure 20 the linear relationship noted in Figure 19 is also noted for a modified abscissa. In Figure 20 the multiplication is illustrated as a function of the ratio of the burnup divided by initial enrichment; once the assemblies are grouped by cooling time we observe that there is little scatter, particularly once the two very low burnup, "starter fuel" assemblies, X and Y, are excluded. Yet, this trend does not hold up as well for the BWR assemblies. It is not clear how these trends will be useful at this time; this discussion is part of the analysis process of looking to exploitable patterns to help predict quantities of interest. In this case we are investigating a relationship among burnup, initial enrichment, cooling time and multiplication.

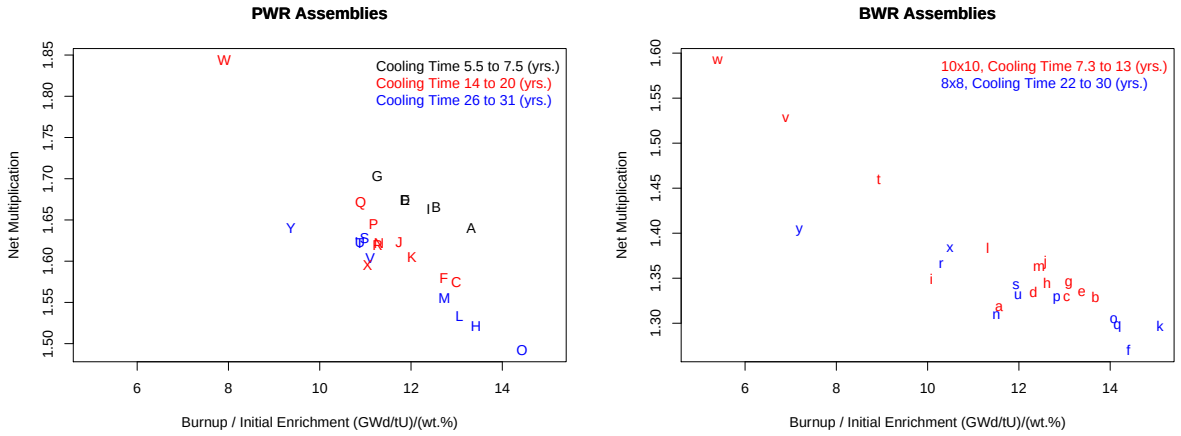

Figure 20: The simulated net multiplication of the PWR (left) and BWR (right) assemblies when situated inside the DDSI instrument is illustrated as a function of the declared burnup divided by initial enrichment.

The following three graphs are an illustration of how patterns might be used to classify assemblies; note these graphs are formed by graphing what will be measured quantities only relative to each other as opposed to the previous three graphs that included declared quantities. In the current cases we are graphing one simulated quantity, multiplication vs. three measured quantities: spectral lines measured with a HPGe detector and the total neutron count rate measured with the Euratom Fork detector. In Figure 21 for the PWRs we observe that the assemblies of a given cooling time group scatter around a negatively sloping line for the multiplication vs. the count rate of the 662 keV line of ^{137}Cs; all except for Assembly X, which behaves very similarly to Assembly Y. For the BWRs we see a similar pattern with no outliers. The physical

explanation for the observed trend is that the more an assembly is irradiated the more the multiplication is reduced and the more ^{137}Cs is produced. The grouping into cooling time groups makes sense as the ^{137}Cs decays with a cooling time that would shift the entire curve to the left. The fact that Assembly X behaves similar to Assembly Y is not surprising as we know that about 83% of the irradiation of Assembly X occurred at the same time as Assembly Y. The 17% of additional irradiation that occurred a decade later is not very significant in producing much ^{137}Cs.

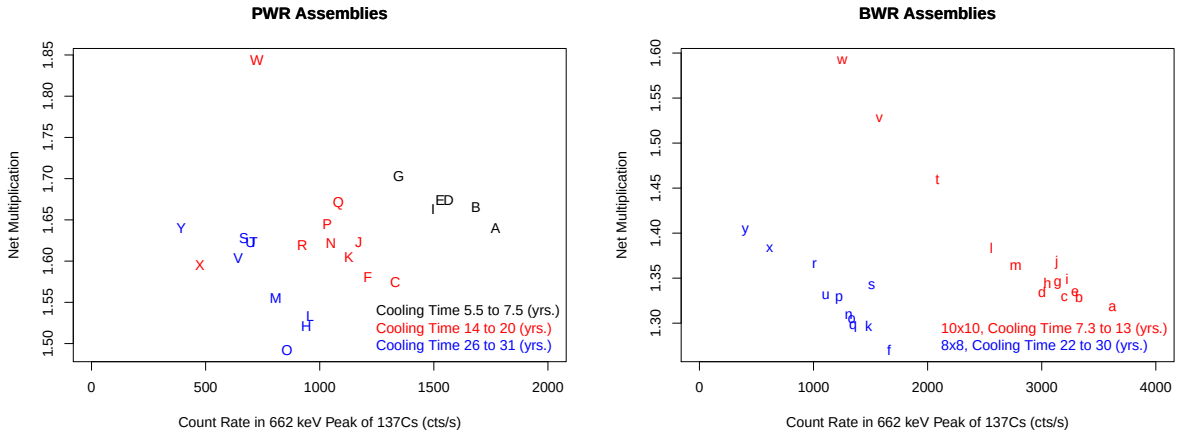

Figure 21: The simulated net multiplication of the PWR (left) and BWR (right) assemblies when situated inside the DDSI instrument is illustrated as a function of the 662 keV line of ^{137}Cs.

In Figure 22 the multiplication is illustrated as a function of the ratio of the 1274 keV line of ^{154}Eu to the 662 keV line of ^{137}Cs. Each cooling time group is observed to stay as a group. Interestingly PWR Assembly X moves into the cooling time group to which it belongs. Perhaps comparing Figures such as 21 and 22 may be a way of diagnosing assemblies that were removed from the reactor for abnormally long time intervals. It is expected that Assembly X moved as it did between these two graphs because (1) ^{154}Eu is produced at twice the rate per unit burnup at the end of a typical assembly's irradiation when ^{239}Pu fissions significantly more than ^{235}U [35] and (2) the 8.6 year half life of ^{154}Eu means that ^{154}Eu atoms produced during the initial "83%" of Assembly X's irradiation interval have decreased by more than a factor of two before the second "17%" irradiation took place, thus emphasizing the presence of the ^{154}Eu atoms produced during the second irradiation of Assembly X.

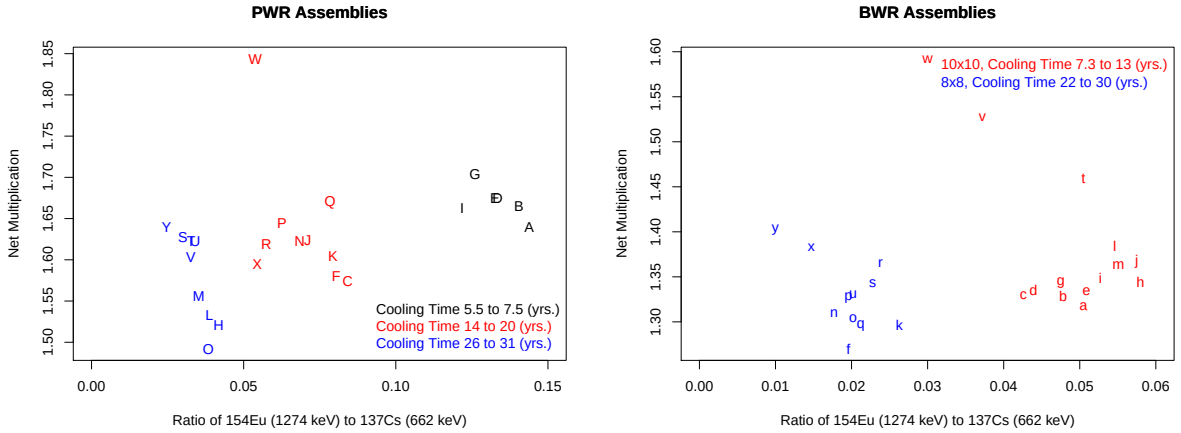

Figure 22: The simulated net multiplication of the PWR (left) and BWR (right) assemblies when situated inside the DDSI instrument is illustrated as a function of the ratio of the count rate for the 1274 keV line of ^{154}Eu to the 662 keV line of ^{137}Cs.

In Figure 23 the multiplication is illustrated as a function of the total neutron count rate. We see that the assembly grouping is very similar to that which was observed in Figure 21. Hence, total neutron could be used instead of the 662 keV line intensity for the purposes discussed in the previous paragraph; or this could be a means of checking for consistency among various NDA signatures which might reveal some diversion scenarios.

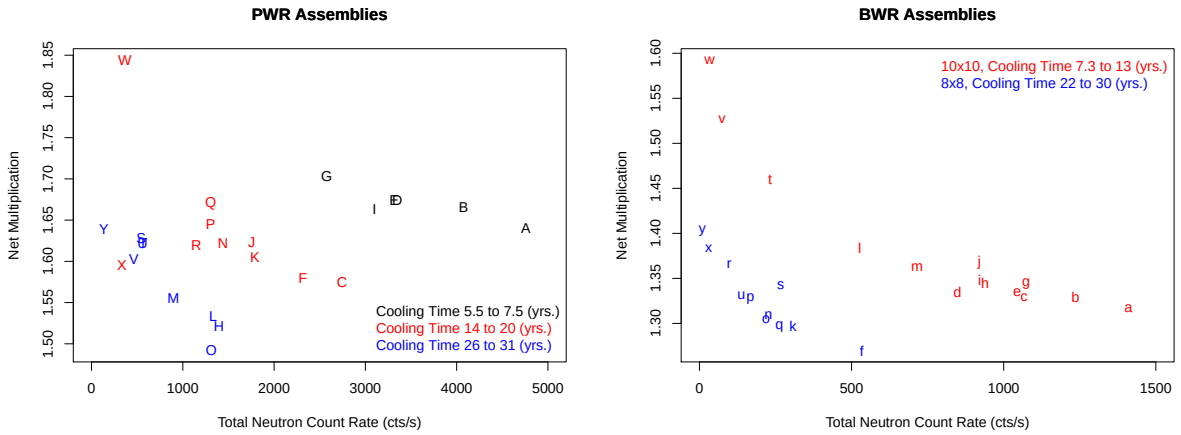

Figure 23: The simulated net multiplication of the PWR (left) and BWR (right) assemblies when situated inside the DDSI instrument is illustrated as a function of the measured total neutron count rate.

11 Integration 7: Spectral Resolved Gamma, Total Neutron, Multiplication and Calorimetry

11.1 Description of the "Raw" Data

Given time limitations, only a couple of graphs are provided below. Many more have been produced but additional time is needed to analyze the results.

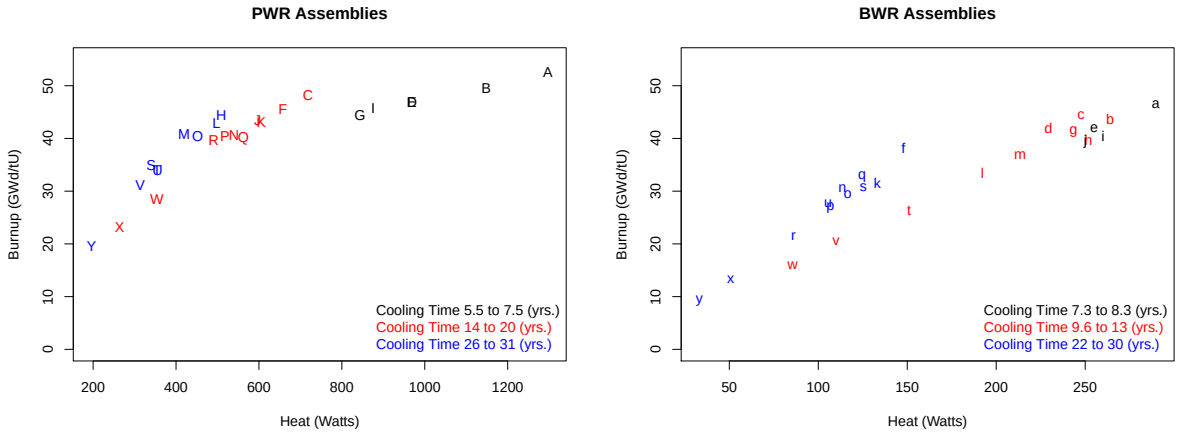

Figure 24: The burnup of the PWR (left) and BWR (right) assemblies is illustrated as a function of the heat simulated with SCALE.

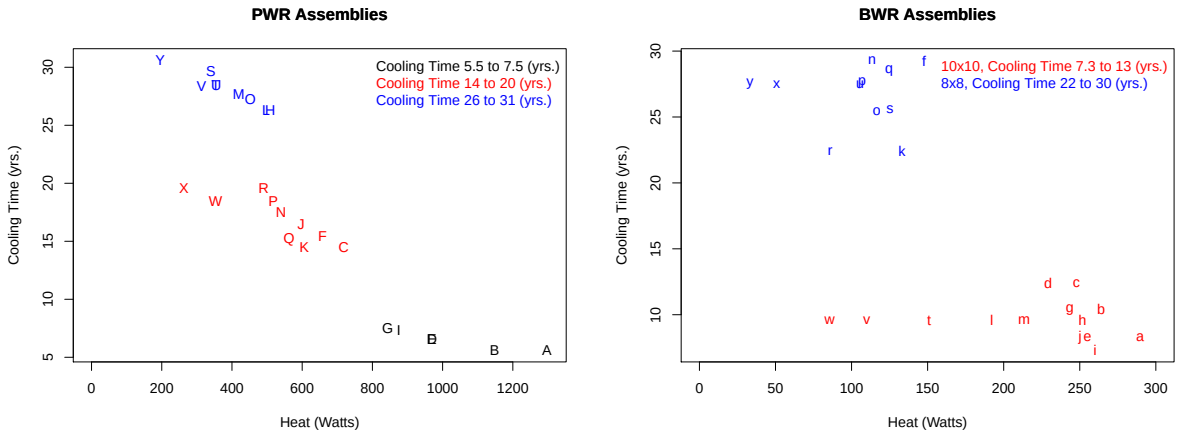

Figure 25: The cooling time of the PWR (left) and BWR (right) assemblies is illustrated as a function of the heat simulated with SCALE.

12 Summary/Conclusions/Next Steps

12.1 Description of Research Context

For the past three years, ever since the SKB-50 assemblies selection process was finalized, which was around the middle of 2014, our research effort has built a database that contains basic assembly information, measured NDA data and simulated data for these assemblies. A summary of that database in its current form is the following:

1. Completed Measurements:
   (a) Euratom Fork - total neutron and gross gamma, and
   (b) Spectral resolved gamma - photons from ^{134}Cs, ^{154}Eu and ^{137}Cs have been the primary focus.
2. Completed Simulations:
   (a) Total Neutron emission (DDSI geometry)
   (b) Heat (SCALE with structural material, some Casmo/Simulate results).
   (c) Pu Mass (Casmo/Simulate/Polka results from Dark data bases, SCALE)
   (d) Multiplication (DDSI geometry)
3. Obtained Assembly Data:
   (a) Initial Enrichment (SKB's Dark and Pluto databases, and ORNL process reactor operator data)
   (b) Burnup (SKB's Dark and Pluto database which contained data from Casmo/Simulate/Polka, and SCALE)
   (c) Cooling Time (Dark database)
   (d) Time in Reactor (time between first loading and final discharge)
   (e) Assembly Type (15x15, 17x17, 8x8, 10x10)
   (f) Presence or Absence of Burnable Poisons
4. Measurements Yet to be Made
5. Data still needed

This FY17 report was an opportunity to explore the large amount of data we have accumulated and look for patterns and explanation for basic patterns. In large part this process involved making well over 100 graphs by selecting one variable as the ordinate and seeing how that variable changed as a function of the other 18 variables or ratio of variables. A subset of the relationships investigated were included in this report.

12.2 Conclusions/Summary and/or Thoughts-in-Process

1. The focus on encapsulation safeguards brings with it factors that strongly impact the NDA system, in particular: (1) Focus on fuel that is 10 to 70 year cooled and (2) Weight of the instrument is not a significant concern, (3) Reliability/robustness is extremely important. (4) Count times that are of approximately 30 minutes or less.

2. The vast majority of the assemblies to be measured will be "fully irradiated" in a roughly systematic manner. It is suggested that the analysis should focus on these assemblies and develop corrections for assemblies that are more or less fully irradiated.

   (a) By "fully irradiated" we mean that each assembly at creation is embedded with potential nuclear energy by virtue of its initial enrichment and assembly structure. The reactor operator is expected to optimally extract this energy over a typical time range. **This reality considerably constrains the potential isotopic variation that typical fuel can experience.** It is important to note that the SKB-50, by the selection process used in the formation of this group, is expected to exhibit greater variation than more typical assemblies.

   (b) Most assemblies of a given fuel type (17x17 or 8x8, etc.), or group of fuel types (17x17 and 15x15) will have similar discharge multiplication values that do not change much in the following decades, see Figures 17 and 19.

   (c) A measurement of multiplication can quantify the degree to which an assembly was fully irradiated or not. The systematic uncertainty of multiplication measurements is a key research question that this research effort will inform.

3. Given the complexity of spent fuel, more assemblies in addition to the SKB-50 assemblies are needed for a robust uncertainty analysis. There need to be enough typical assemblies to quantify signals variation for typical assemblies before atypical assemblies can be properly researched. In the context of "groups," the first level of division is between PWR and BWR reactor types; these will then need to be subdivided as in the case of BWRs into 11 8x8s and 14 10x10s. Additionally there need to be enough atypical assemblies in each group to quantify how they vary. It is anticipated that groups can be combined through correction factors but it is expected that groups will need to be understood separately first. Simulations have a clear role to play here but it is important that the simulated assemblies very nearly match, or are perturbations of, the realistic fuel expected to go into the repository.

4. The current research effort is expected to provide evidence, positive or negative, with respect to the benefits for inclusion of NDA capability beyond the already anticipated total neutron and spectral resolved gamma capability anticipated for Clink.

12.3 Suggested Next Steps in Analysis

1. Complete Integrations 1 and 2 for all the research objectives. All the data exists and much of the exploratory research has been done. Much of the data is presented in this report but a focused subsection should be written up on each goal. From past research it is recommended that not much effort be expended on model formation with Integration 1 beyond how total neutron and gross gamma vary with the key variables. Our research to date indicates that producing models beyond simple data correlation is not warranted.

2. Focus on a **data justified,** cooling time correction.

   (a) Frequently in spent fuel NDA research the declared cooling time is used to correct the data back to discharge or some other date that allow cooling time independent comparison among assemblies. By "data justified" we mean that some measured signal such as the ratio ^{154}Eu to ^{137}Cs must be used; related to this some verification that the assembly is "fully irradiated" may also be needed. The limits of this justification need to be quantified to justify the merit of this approach. Research

into and “effective cooling time” as well as the accurately defined cooling time are encouraged.

(b) A few words on the philosophical motivation for focusing on cooling time: What takes place in a reactor is very complex as evidenced by the complexity of the codes needed to simulate reactor operation (Casmo/Simulate, SCALE, Monteburns, etc.). What takes place after leaving the reactor is simple, exponential decay of isotopes that exist independent of each other. The inaccuracy of cooling time correction are essentially due to uncertainty in what was created when in the reactor. The cooling time correction allows us to focus on what provides the greatest uncertainty in our effort.

3. Incorporate new experimental results as available.

13 Appendix A: Relative Roles of Measured and Simulated Data

The paragraphs in this section that follow this paragraph are from the FY15 year end report. They are included here as a place marker to remind a future author to update the text to reflect lessons learned. One main lesson learned in FY16 was described in the INMM paper by Tobin et al.[37] which was that **we have to be careful in how we use simulation to augment experimental data.** Virtual assemblies that were created for the purpose of testing the capability of various NDA techniques are not expected to be appropriate for estimation of how an integrated NDA system will perform. The point is somewhat subtle. In the case of commercial assemblies, the reactor operator is focused on optimally using the potential nuclear energy in each assembly. As such, **the overwhelming majority of assemblies of a given initial enrichment are irradiated to a relatively narrow specific burnup range.** This reality is anticipated to make the task of pattern identification easier as the range of possible outcomes is limited by economic constraints. Furthermore, the role of multiplication was elevated in this context because multiplication can quantify how close any given assembly is to the optimal irradiation, detecting over or under irradiation. In contrast **the assemblies we simulated as a part of this project's down-selection process were not created with the final interpretation of measured data in mind.** As such the connection between initial enrichment and final burnup was only very roughly connected to that observed for commercially irradiated fuel. For this reason, it is not clear at this time if the use of past simulations can be used in future analysis or if such use will significantly bias any conclusion that might be reached.

Text from the FY15 report:

The purpose of this report is to inform decisions in the context of how well each of several NDA systems can, or cannot, meet each of 5 different technical goals for several scenarios with respect to the use of declared data. The initial analysis involves examining what can be concluded from measured data alone and then building on the measured data by including declared data. Inherent in researching this approach is the need for the measured data to span the full range of parameter space that impacts the NDA signals. In this section the degree to which the SKB-50 assemblies span the parameter space of interest to our 5 technical goals is discussed. To inform this discussion, research performed on simulated PWR spent fuel libraries [5]

are used.

In the full safeguards context, all spent fuel from all reactors from discharge to around 70 years of cooling is of current research interest. Yet, in the context of this report, we are looking at a subset of this larger parameter space by focussing on the fuel and research questions of relevance to the Swedish repository. Hence, the range of interest includes PWR and BWR fuel with cooling times between 10 and about 60 years; fortunately this reduced parameter space includes a large fraction of all the spent fuel under international safeguards.

It is evident that the current measured database formed by the SKB-50 assemblies is limited in two key aspects: (1) The fuel types going into the Swedish repository are more diverse than the two BWR (8x8 and 10x10) and the two PWR fuel types measured (15x15 and 17x17). Additionally, due to the absence of neutron data for the PWRs the current report only has a complete data set for the BWR assemblies. (2) The range of cooling times of the BWR assemblies is particularly limited with one cooling time grouping of between 22 and 29 years; additionally all of these long cooled assemblies are 8x8 assemblies and no 8x8 assemblies were measured with cooling times outside of this range. A second group with cooling times between 7 and 12 years was measured; all of these assemblies are 10x10. Hence, there are approximately two cooling times for all the BWR assemblies and each of these cooling times are for one fuel type.

In Figures 26 and 27, the experimental data for the 25 BWR assemblies analyzed in the previous section are plotted along with simulated data for several PWR assemblies from two different simulated spent fuel libraries used during the NGSI-SF Project [5]. In making this graph a multiplicative constant was used to adjust the simulated ion chamber gamma intensity so that both data sets are on the same scale. The magnitude of this constant was calculated by taking the ratio of the experimental measured ion chamber gamma intensity for "Assembly a" (initial enrichment 3.14%, burnup 46.4 GWd/tU and cooling time 8.3 years) to the simulated ion chamber gamma intensity of an assembly with initial enrichment 4.0%, burnup 45 GWd/tU and cooling time 5 years.

The motivation for making Figures 26 and 27 was to illustrate that once normalized, the simulated burnup and gross gamma trend in a similar way to the measured data for the parameter space where they overlap. Note that if such a normalization were used in practice additional study is needed to show how

results vary depending on which assembly is selected for normalization. Ideally, the simulation results would use one of the assemblies in the measured data set but this was not done for the current analysis. The first step in producing simulated NDA signals from the NDA instruments is simulating the reactor irradiation; research that is ongoing and to be published soon [38].

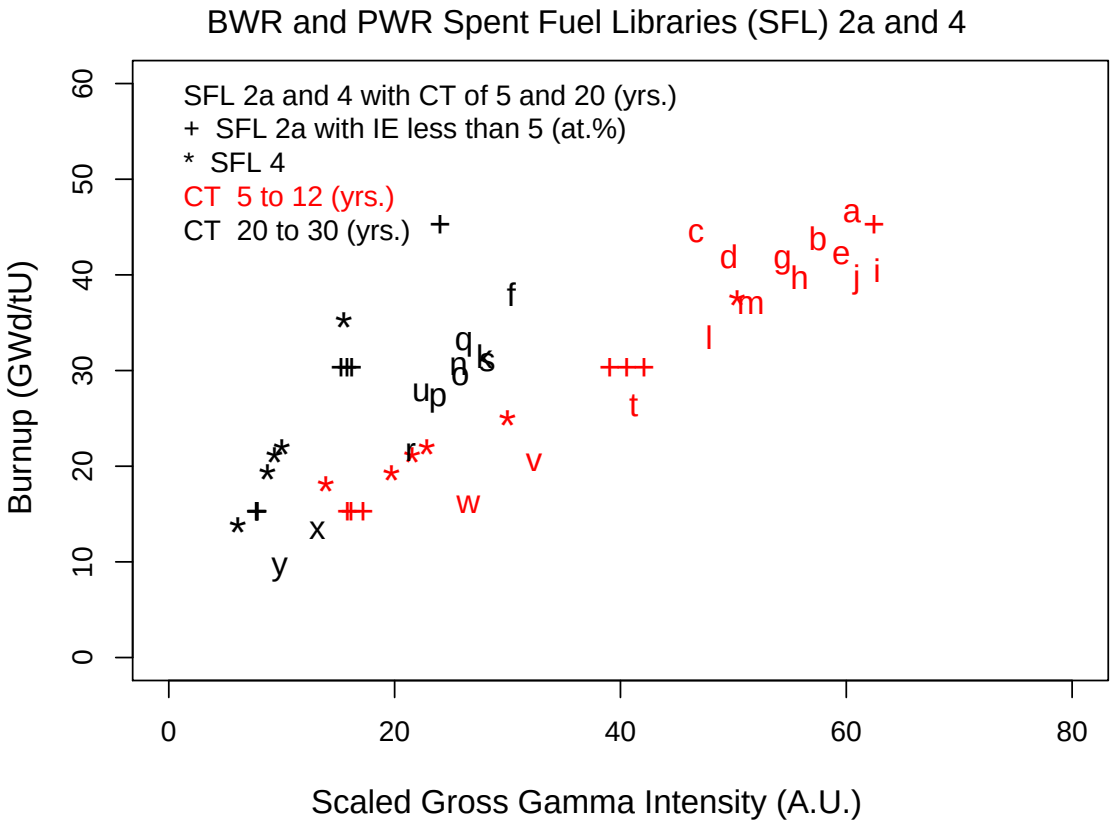

Figure 26: Co-plot of the gross gamma intensity as a function of burnup for both experimentally measured BWR assemblies indicated with letters of the alphabet and the simulated PWR assemblies indicated with astrix and plus symbols.

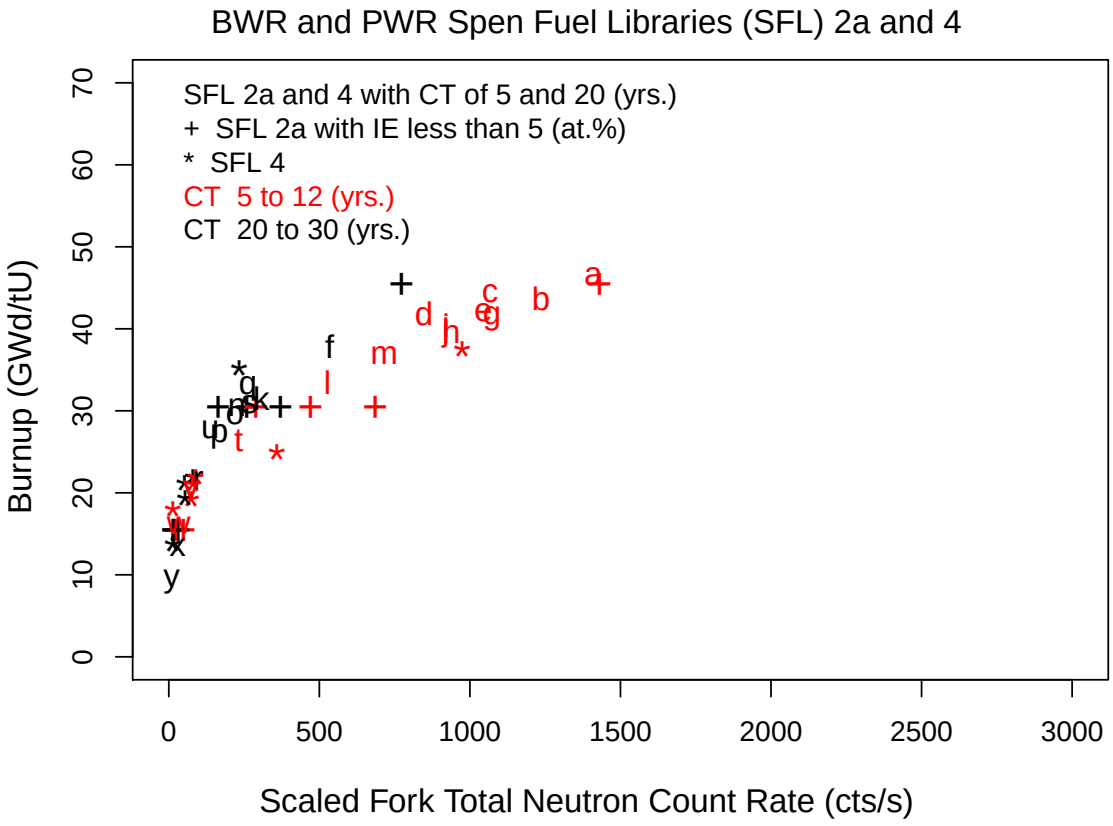

Figure 27: Co-plot of the total neutron intensity as a function of burnup for both experimentally measured BWR assemblies indicated with letters of the alphabet and the simulated PWR assemblies indicated with astrix and plus symbols.

Given the general agreement between simulation and measurements depicted in Figures 26 and 27, we have some confidence in using more simulated data from the same simulated dataset to extrapolate into the parameter space not covered by the experimental data. The data that may allow us to extrapolate into a broader parameter space is illustrated in Figures 28, 29 and 30.

In Figure 28 the cooling time as a function of gross gamma intensity for simulated PWR assemblies is illustrated. Each frame is a different initial enrichment value and color is used to separated assemblies of different cooling times. Assemblies from Spent Fuel Libraries SFL-2a and SFL-4 were selected. The main point to take away from Figure 28 is how little initial enrichment matters to the simulated gross gamma signal; this is perhaps best illustrated by noting how the red curve is nearly identical as a function of initial enrichment. Another point to note is that the change in the gross gamma count rate is more dynamic between the cooling times of 5 and 20 years than between the cooling times of 20 and 40 years. At 5 years cooling time both ^{134}Cs and ^{137}Cs contribute significantly to the gross gamma signal while at 20 years and beyond, only ^{137}Cs is a significant source. The usefulness of Figure 26 is that it enables us to visualize the change in the gross gamma intensity over the entire cooling time range of interest to our project.

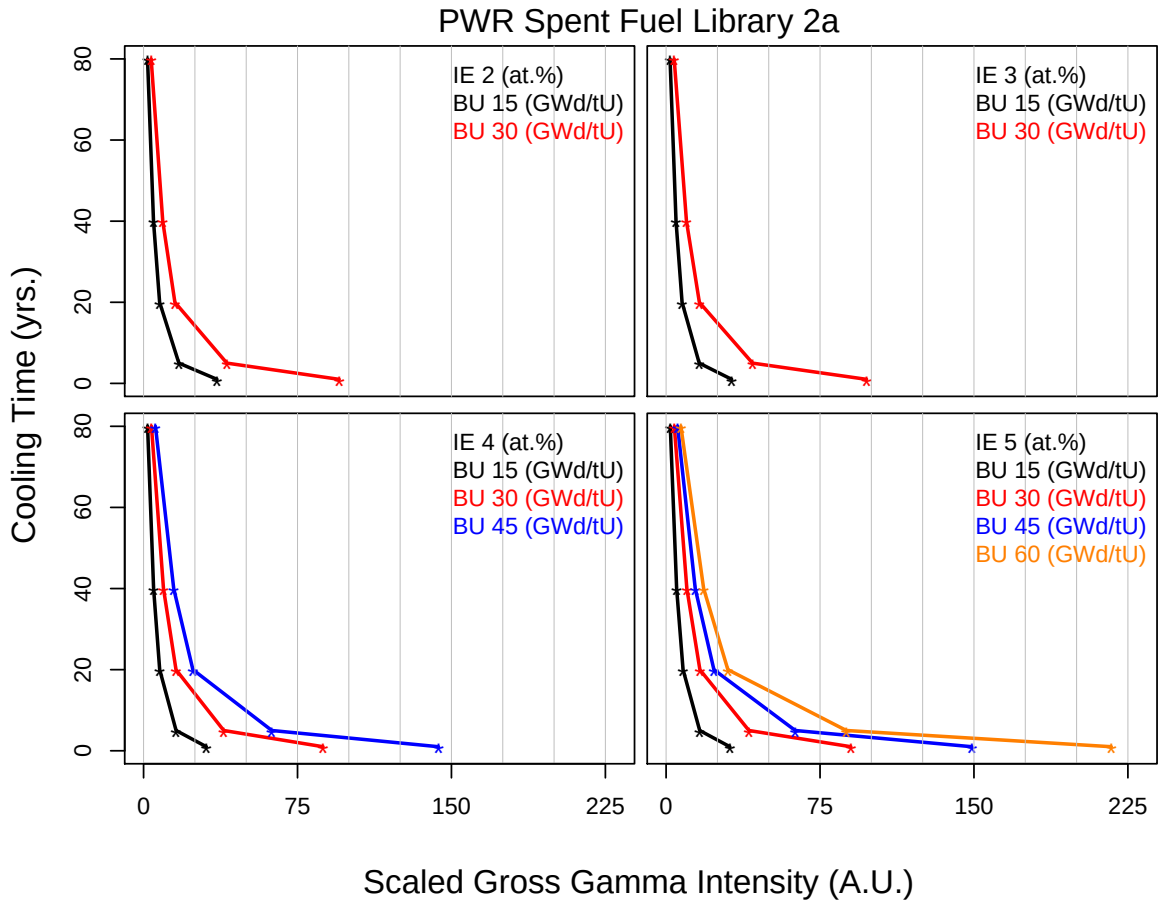

Figure 28: The cooling time dependence of the scaled gross gamma intensity for simulated PWR assemblies is illustrated for four different initial enrichments and for four different burnups.

In Figures 29 and 30 the interdependence among the initial enrichment, burnup and cooling times in terms of how each parameter impacts the total neutron count rate is depicted; note the data in both figures is identical, two figures were made to better enable visualization of this dynamic, interrelated data. As with previous graphs, the number of data points within a given sub-figure was dictated by the practicality that a given initial enrichment will only be irradiated to a given burnup level. The very strong dependence of the total neutron count rate on burnup as well as lesser dependences on initial enrichment and cooling time are all evident.

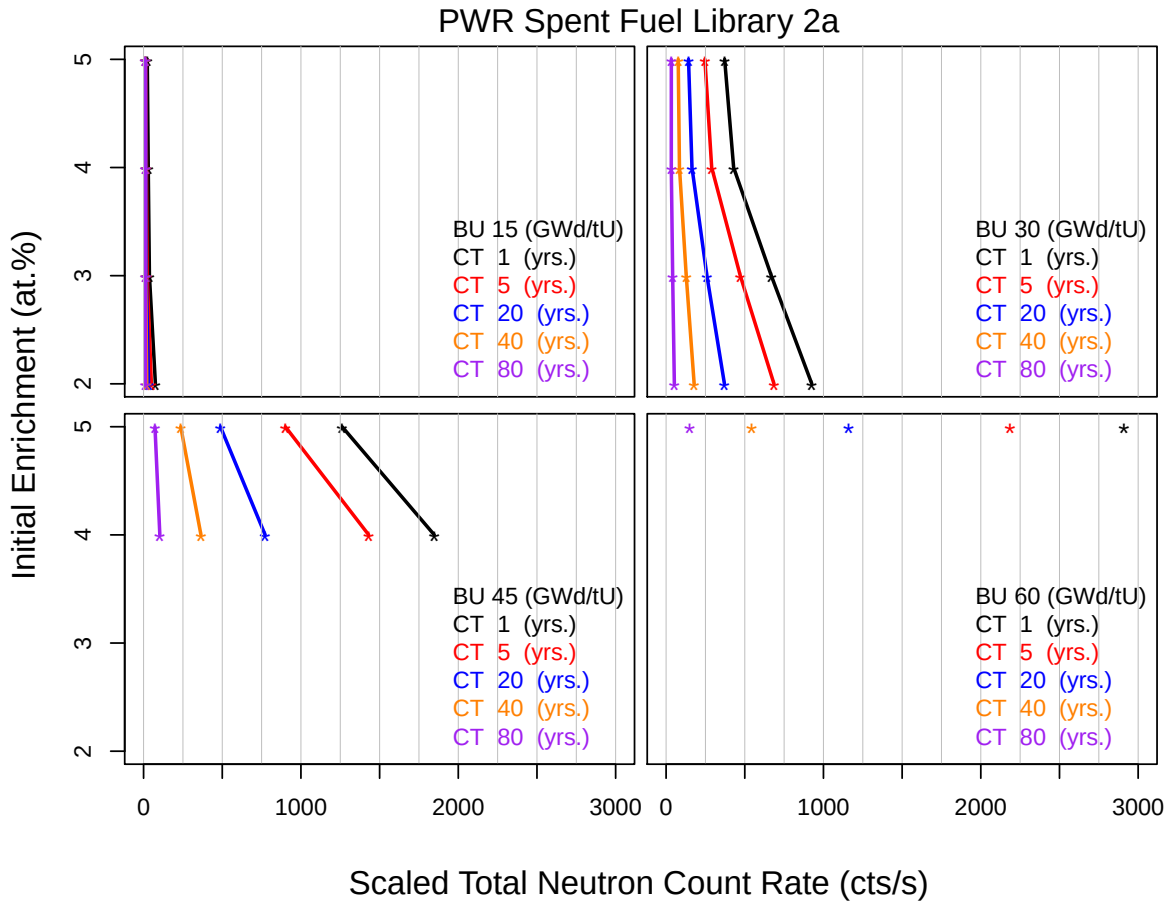

Figure 29: The assembly initial enrichment is illustrated as a function of the total neutron count rate with four different graphs, a different graph for each burnup. Color was used as a means of separating the count rate for different cooling times.

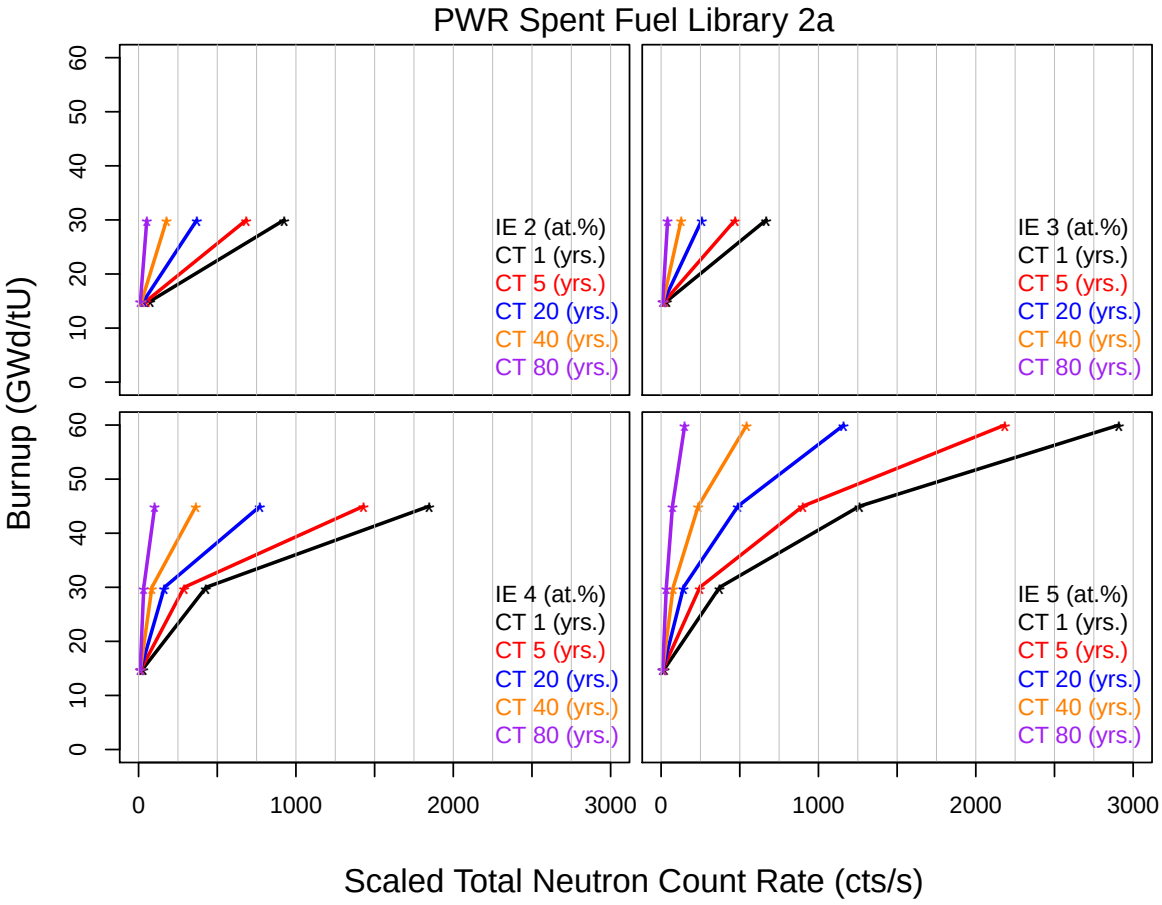

Figure 30: The assembly burnup is illustrated as a function of the total neutron count rate with four different graphs: a different graph for each initial enrichment. Color was used as a means of separating the count rate for different cooling times.

13.1 Estimation of Initial Enrichment, Burnup and Cooling Time Using Gross Gamma and Total Neutron Signals Only - No Declared Data

The research on model development is premature at this point. The majority of the effort on data mining involved working with and understanding the quality and limitations of the dataset. However, in Figure 31 a preliminary prediction of the burnup level is given for some of the initial model formation research. A Bayesian Tree model was used. The algorithm was formulated with information from the BWR and PWR

spent fuel libraries 2a and 4 as well as using the simulated gross gamma and total neutron signals obtained for the 2a and 4 PWR libraries. The simulated and measured data were combined by adjusting the measured gross gamma intensity and the total neutron count rates as described in the section on "Relative Roles of Measured and Simulated Data;" Assembly a of the SKB-50 BWR assemblies was assumed to be the same as a similar assembly in the simulated library for normalization purposes. The predicted burnup is graphed as a function of the declared burnup in Figure 31; a calculation that used the gross gamma and total neutron data measured with the Fork detector as input. A root-mean-square prediction error (RMSE) of 3.11 GWd/tU was estimated; the RMSE is an indication of the spread in the data around the curve fit to the data set, in other words a kind of generalized standard deviation.

Note that this use of simulated data and measured data is a large research question in and of itself, but at this point it is simply offered as a sample of potential research avenues moving forward. One option being considered is to use the simulated data to create an algorithm and then to test the algorithm with the measured data. Biases are anticipated to exist between the simulated and measured data. The second step in the process would be to modify the simulation formulated algorithm to correct for some of the biases noted in the experimental data. In so doing, some of the limitation of the experimental data, such as not enough cooling time variability, may be corrected.

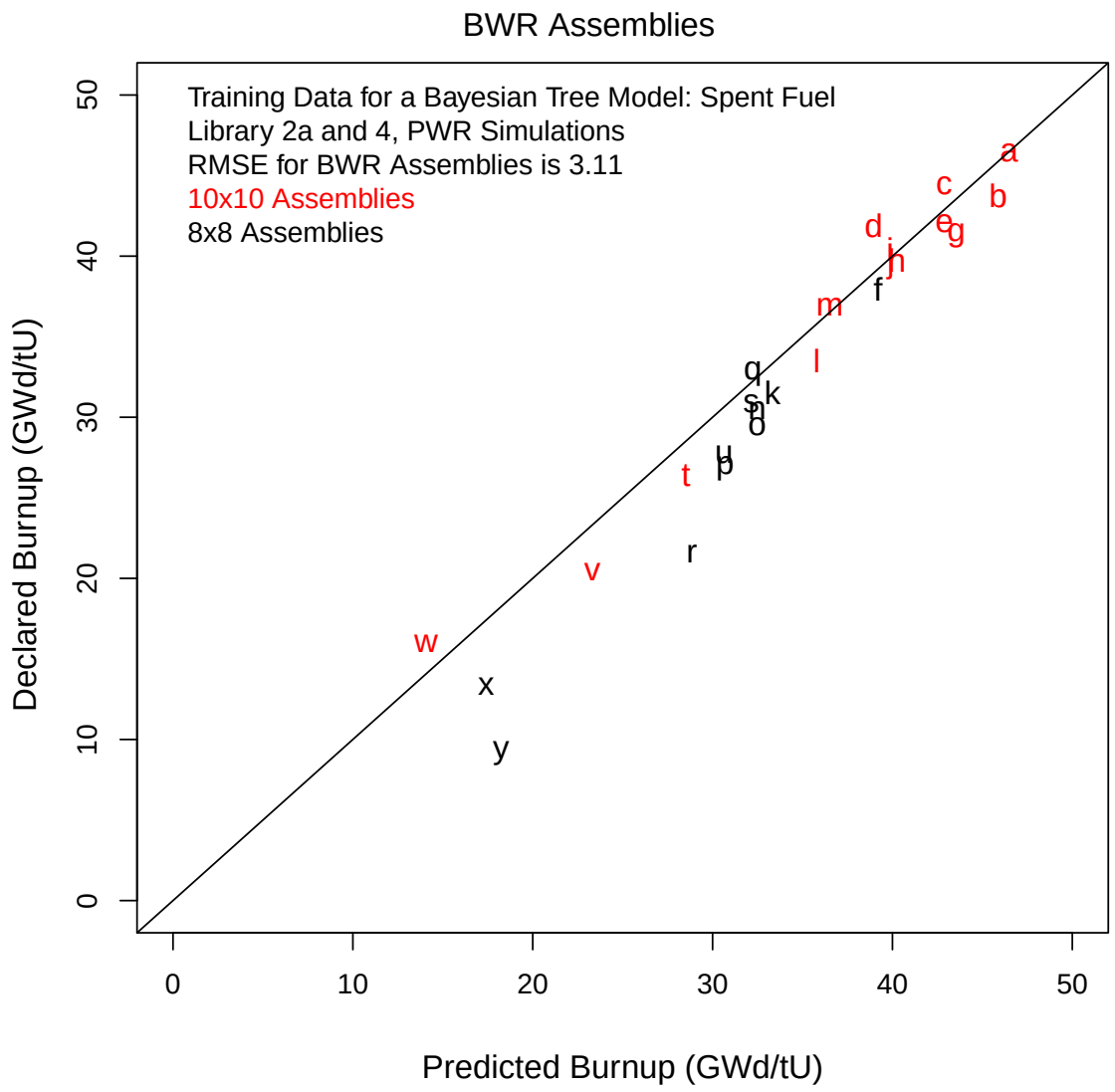

Figure 31: The burnup value calculated by the reactor operator is graphed vs. the burnup predicted for each assembly using a Baysian Tree Model that was trained on simulated results from BWR and PWR spent fuel libraries 2a and 4. [5]

14 Appendix B: Comparison among Passive Gamma Data

It is important to check the quality of the experimental data both by benchmarking with simulations and by comparison among datasets as applicable. As more instruments are deployed, comparisons among experimental instruments will be made in this section.

We did not intend to perform two separate passive gamma measurement campaigns for both the PWR and BWR assemblies; but such was the reality due to hardware malfunctions during the first two campaigns at Clab. This situation resulted in some approximately duplicated data being collected. In this section and in the publication by [8] this duplication is taken advantage of as a chance to check the reliability of our data. A comparison between two different HPGe detectors is illustrated in Figures 32 and 33 for both the PWR and BWR assemblies. Note that the axial locations measured were 120 cm apart in the case of the PWR assemblies and 15 cm apart for the BWR assemblies, facts which are expected to be the cause of the majority of the scatter in the data points.

The experimental system used in the first two measurement campaigns was provided by Lawrence Livermore National Laboratory; it was an Ortec GMX detector. A Canberra Lynx was used as the multichannel analyzer, the data from which is graphed on the horizontal axis of Figures 32 and 33 . The experimental system provided by Euratom was a Canberra GX detector and a digital MCA-527 by GBS Elektronics the data from which is graphed on the vertical axis.

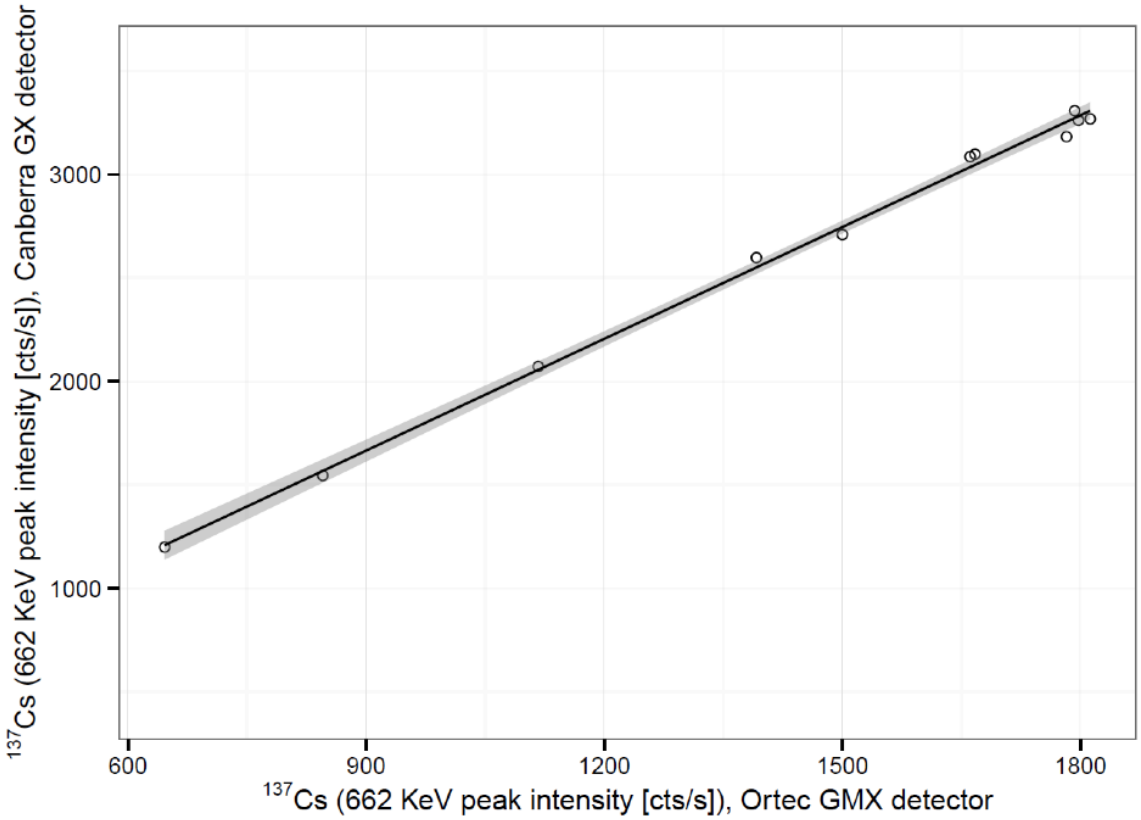

Figure 32: Comparison of the measured 662 keV peak count rate from 137Cs as measured from the same corner of several of the BWR assemblies for the two experimental systems described in the text.

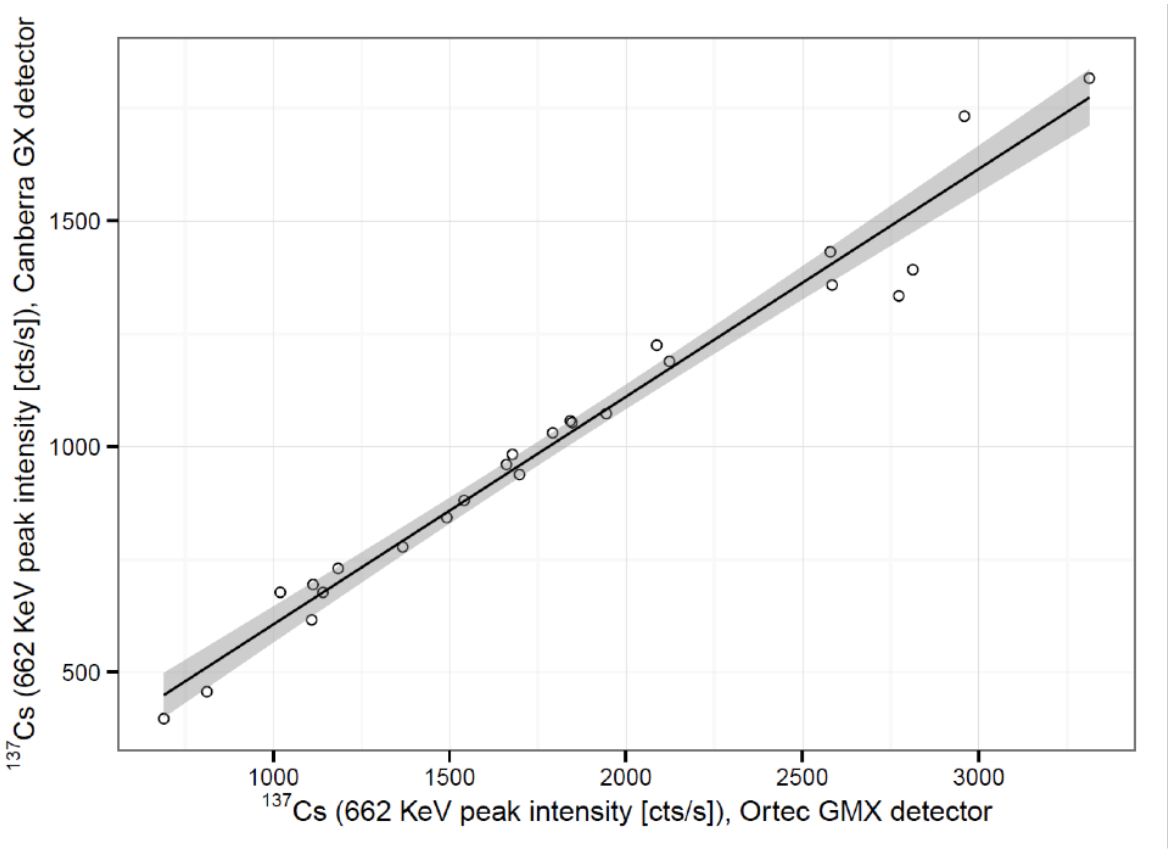

Figure 33: Comparison of the measured 662 keV peak count rate from 137Cs as measured from the same corner of several of the PWR assemblies for the two experimental systems described in the text.

15 Appendix C: Measured and Simulated Passive Gamma Data

To be completed in FY16 or later provided sponsor supports this research path. As of the writing of this report, the simulation of the SKB-50 assemblies with the detailed reactor operating data is nearly completed. Such work is a precursor to performing the NDA simulations.

16 Appendix D: Comparison among Total Neutron Data

Paul De-Baere of Euraom is the subject matter expert for the Fork instrument at Euratom. He provided the following text in the context of how the BWR Fork detector operated during measurements at Clab during March of 2015:

"One of the neutron channels (ChA) of the BWR fork showed erratic spurious counting, sometimes a bit (not too disturbing) or huge (through the ceiling). Channel B always worked fine. For that reason, I sometimes had to select a small good part of the data in a few assemblies. A few times the event was so ruined by the spurious counting that I had to calculate ChA from ChB with the "channel ratio" of 2.529 (empirically defined from 22 measurements).

The second day, we started with the remaining 2 elements (assemblies) and then tried to re-measure five elements (assemblies) that suffered from the spurious counting (in day 1). The neutrons agreed well to the previous day, but the gammas on those were exactly 13% lower. Why is still unclear."

An additional point worth noting in the context of the Fork detector measurements. For the measurements used in this report, the researcher operating the Fork was on a bridge crane. From that position the individual deploying the Fork pulled back on the pole so that the polyethylene of the "cusp" of the Fork rested against the assembly. This minimized the positioning uncertainty. For a final unattended deployment, it is more likely that an actual Fork detector would be installed on the side of a pool. In this situation, the crane operator would bring the fuel into the Fork most likely from the side. The operator would most likely stop before the Fork was incident upon the polyethylene "cusp" section of the Fork. Hence, increasing the systematic uncertainty.

17 Acknowledgements

This work was performed in the framework of the collaboration agreement (Action Sheet 50 under the U.S. DOE-EURATOM cooperation agreement) among the Swedish Nuclear Fuel and Waste Management Company (SKB AB), the European Commission and the Office of Nonproliferation and Arms Control (NPAC), National Nuclear Security Administration (NNSA). The personnel at the interim storage facility for spent nuclear fuel (Clab) in Oskarshamn, Sweden, are acknowledged for their support.

References

[1] M.A. Humphrey, S.J. Tobin, and V.D. Veal. The next generation safeguards initiative's spent fuel nondestructive assay project. *Journal of Nuclear Material Management*, 40(3):6–11, 2012.

[2] S.J. Tobin, H. Liljenfeldt, H. Trellue, G. Baldwin, A. Belian, D. Blair, T. Burr, P. De-Baere, M. Fensin, A. Favalli, J. Galloway, I. Gauld, S. Grape, B. Grogan, Y. Ham, J. Hendricks, V. Henzl, J. Hu, K. Ianakiev, G. Ilas, P. Jansson, A. Kaplan, T. Martinik, H. Menlove, D. Meyers, V. Mozin, M. Newell, P. Polk, C. Rael, S. Pozzi, P. Santi, P. Schwalbach, A. Sjöland, S. Jacobsson Svörd, M. Swinhoe, T.J. Ulrich, S. Vaccaro, D. Vo, and A. Worrall. Experimental and analytical plans for the non-destructive assay system of the swedish encapsulation and repository facilities. *Proceedings of International Atomic Energy Agency Symposium on International Safeguards: Linking Strategy, Implementation and People*, October 2014. IAEA-CN-220-238.

[3] P.M. Rinard and G.E. Bosler. Safeguarding lwr spent fuel with the fork detector. Report LA-11096-MS, Los Alamos National Laboratory, 1988.

[4] A. Borella, R. Carchon, C. DeLimette, D. Symens, and K. van der Meer. Spent fuel measurements with the fork detector at the nuclear power plant of doel. *ESARDA 33rd annual meeting, Budapest, Hungary, and Publications Office of the European Union*, (ISBN 978-92-79-18525-0), 16-20 May 2011.

[5] H.R. Trellue, J.D. Galloway, N.A. Fischer, and Tobin S.J. Advances in spent fuel libraries. *Proceedings of Institute of Nuclear Materials Management conference, Palm Desert, California*, (LA-UR-13-24074), July 2013.

[6] T. Burr, H.R. Trellue, S.J. Tobin, A. Favalli, J. Dowell, V. Henzl, and V. Mozin. Integrated nondestructive assay systems to estimate plutonium in spent fuel assemblies. *Nuclear Science and Engineering*, 179:321–332, 2015.

[7] H.R. Trellue, D.I. Poston, S.J. Tobin, and Y. Ham. The use of non destructive assay measurements to estimate burnup and plutonium inventory in pressurized water reactor spent fuel assemblies. Report LA-UR-13-27521, Los Alamos National Laboratory, 2013.

[8] S. Vaccaro, S.J. Tobin, A. Favalli, B. Grogan, P. Jansson, H. Liljenfeldt, V. Mozin, J. Hu, P. Schwalbach, A. Sjöland, H. Trellue, and D Vo. Overview of passive gamma measurements of spent fuel assemblies with a high purity germanium detectors at the central interim storage facility for spent nuclear fuel in sweden. Report LA-UR-15-23993, Los Alamos National Laboratory, 2015. Expect to publish in NIM-A.

[9] Jansson et al. Axial and azimuthal gamma scanning of nuclear fuel - implications for spent fuel characterization. *TBD*, 2015.

[10] B.R. Grogan, A. Favalli, P. Jansson, V. Mozin, P. Schwalbach, A. Sjöland, S.J. Tobin, H.R. Trellue, S. Vaccaro, and D. Vo. Nda measurement analysis of spent nuclear fuel assemblies at the swedish clab facility using the indepth code. *Institute of Nuclear Material Management*, July 2016.

[11] D. Vo, A. Favalli, B. Grogan, P. Jansson, H. Liljenfeldt, V. Mozin, P. Schwalbach, A. Sjöland, S.J. Tobin, H. Trellue, and S. Vaccaro. Determination of initial enrichment, burnup and cooling time of pressurized-water-reactor spent fuel assemblies by analysis of passive gamma spectra measured at the clab interim-fuel storage facility in sweden. *Proceeding of the Institute of Nuclear Material Management*, 2015. LA-UR-15-24252.

[12] A. Favalli, D.W. Lee, J. Hu, S.J. Tobin, and H.R. Trellue. Determination of initial enrichment, burnup, cooling time of pwr spent fuel assemblies by analysis of passive gamma spectra and neutron count rate. *Los Alamos National Report, LA-UR-13-27537*, 2013.

[13] A. Favalli, S. Brambilla, S. Croft, M.L. Fensin, N. Fisher, J. Galloway, J. Gerhart, J. Hendricks, D.W. Lee, M.A. Schear, M.T. Swinhoe, S.J. Tobin, and H.R. Trellue. On determination of initial enrichment, burnup, cooling time of the pwr spent fuel assemblies analysis of passive gamma spectra and neutron count rate. *Institute of Nuclear Material Management, Orlando, Florida USA*, July 15-19, 2012.

[14] A. Favalli, D Vo, , B. Grogan, P. Jansson, H. Liljenfeldt, V. Mozin, P. Schwalbach, A. Sjöland, S.J. Tobin, H. Trellue, and S. Vaccaro. Determining initial enrichment, burnup, and cooling time of pressurized-water-reactor spent fuel assemblies by analyzing passive gamma spectra measured at the clab interim-fuel storage facility in sweden. *Nuclear Instruments and Methods A*, 820:102–111, 2016.

[15] H.O. Menlove, S.H. Menlove, and S.J. Tobin. Fissile and fertile nuclear material measurements using a new differential die-away self-interrogation technique. *Nuclear Instrument Methods in Physics Research Section A: Accelerators, Spectrometers, Detectors and Associated Equipment*, 602(2):588–593, April 2009.

[16] A.C. Kaplan, V. Henzl, H.O. Menlove, M.T. Swinhoe, A.P. Belian, M. Flaska, and S.A. Pozzi. Determination of total plutonium content in spent nuclear fuel assemblies with the differential die-away self-interrogation instrument. *Nuclear Instrument Methods in Physics Research Section A: Accelerators, Spectrometers, Detectors and Associated Equipment*, 764(1):347–351, 2014.

[17] M.A. Schear, H.O. Menlove, S.J. Tobin, L.G. Evans, and S. Croft. Development of the differential die-away self-interrogations technique for spent fuel characterization. Report LA-UR-11-00352, Los Alamos National Laboratory, 2011.

[18] D.M. Lee and L.O. Lindquist. Self-interrogation of spent fuel. Report LA-9494-MS, Los Alamos National Laboratory, 1982.

[19] H.O. Menlove and D.H. Beddingfield. Passive neutron reactivity measurement technique. Report LA-UR-97-2651, Los Alamos National Laboratory, 1997.

[20] J.L. Conlin, S.J. Tobin, J. Hu, T.H. Lee, and H.O. Menlove. Passive neutron albedo reactivity with fission chambers. Report LA-UR-11-00521, Los Alamos National Laboratory, 2010.

[21] J. Eigenbrodt, S.J. Tobin, W.S. Charlton, A.M. Bolind, H.O. Menlove, M. Seya, and H.R. Trellue. Passive neutron albedo reactivity measurements of fugen fuel,. *Atlanta, GA: Proceedings of Institute of Nuclear Material Management*, 2014.

[22] A. Hakansson and O. Osifo. Rapport. CLAB Dokumentreg.nr. 2004-05604, Uppsala University, May 2004.

[23] Svensk Krnbrnslehantering AB. Measurements of decay heat in spent nuclear fuel at the swedish central interim storage facility. Report R-05-62, Svensk Krnbrnslehantering AB, December 2006. Available at http://www.skb.se/upload/publications/pdf/R-05-62.pdf.

[24] V. Henzl, M.T. Swinhoe, S.J. Tobin, and H.O. Menlove. Measurement of the multiplication of a spent fuel assembly with the differential die-away method within the scope of the next generation safeguards initiative spent fuel project,. *Journal of Nuclear Material Management*, 40(3):61–69, 2012.

[25] T. Lee, S.J. Tobin, H.O. Menlove, M.T. Swinhoe, and T.H. Lee. Determining the pu mass in leu spent fuel assemblies: Focus on differential die-away technique. Report LA-UR-11-00747, Los Alamos National Laboratory, 2011.

[26] T. Martinik, V. Henzl, S. Grape, S. Jacobsson Svörd, P. Jansson, M.T. Swinhoe, and S.J. Tobin. Simulation of differential die-away instruments response to active interrogation of asymmetrically burned spent nuclear fuel. *Nuclear Instrument Methods in Physics Research Section A: Accelerators, Spectrometers, Detectors and Associated Equipment*, 788(11), July 2015.

[27] J. Hu, S.J. Tobin, H.O. Menlove, S. Croft, M.T. Swinhoe, M.L. Fensin, T.H. Lee, and J.L. Conlin. Assessment of the californium interrogation prompt neutron (cipn) technique for the next generation safeguards initiative spent fuel research effort. Report LA-UR-11-06890, Los Alamos National Laboratory, 2011.

[28] D. Henzlova, C.D. Rael, H.O. Menlove, R.M. Zedric, J.S. Hendricks, J. Hu, I.P. Martinez, S.J. Tobin, H.R. Trellue, and R.A.J. Weldon. Performance evaluation of californium interrogation prompt neutrons (cipn) technique using fresh and spent nuclear fuel. *IEEE Nuclear Science Symposium, Seattle*, (LA-UR-14-23294), 2014.

[29] J. D. Chen. Detection of partial defects using a digital cerenkov viewing device. *IAEA Symposium on International Safeguards: Preparing for Future Verification Challenges*, 2010.

[30] S. Grape, S. Jacobsson-Svörd, and B. Lindberg. Verifying nuclear fuel assemblies in wet storages on a partial defect level: A software simulation tool for evaluating the capabilities of the digital cherenkov viewing device. *Nuclear Instrument Methods in Physics Research Section A: Accelerators, Spectrometers, Detectors and Associated Equipment*, 698:66–71, 2012.

[31] ORNL Team. Scale: A modular code system for performing standardized computer analysis for licensing evaluations. Report ORNL/TM-2005/39, Version 5, Vols. I-III, April 2005, Available from Radiation Safety Information Computational Center at ORNL as CCC-725, 2005.

[32] Svensk Krnbrnslehantering AB. Technical Report Accessed 21 10 1013, Svensk Krnbrnslehantering AB. Available at http://www.studsvik.com/en/Business-Areas/Operating-Efficiency/Nuclear-Fuel-Analysis-Software/In-Core-Fuel-Management/SIMULATE5/.

[33] T. Goorley. Initial mcnp6 release overview. *Nuclear Technology*, 180:298–315, 2012.

[34] D. Reilly, N. Ensslin, H. Smith, and S. Kreiner. Passive nondestructive assay of nuclear materials. *U.S. Nuclear Regulatory Commission*, 1991. NRC FIN A7241.

[35] J. Hu, I.C. Gauld, J. Banfield, and S. Skutnik. Developing spent fuel assembly standards for advanced nda instrument calibration - ngsi spent fuel project. Report ORNL/TM-2013/576, Oak Ridge National Laboratory, February 2014.

[36] C. Willman. Applications of gamma ray spectroscopy of spent nuclear fuel for safeguards and encapsulation. Ph.D. Report ISSN 1651-6214, ISBN 91-554-6637-0, Uppsala Universitet, 2006.

[37] S.J. Tobin, M.L. Fugate, H.R. Trellue, T.L. Burr, P. De-Baere, P. Jansson, P. Schwalbach, A. Sjöland, and S. Vaccaro. Integration of measured and simulated nondestructive assay data to address the spent fuel assay needs of nuclear repositories. *Institute of Nuclear Material Management*, July 2016.

[38] J. Hu. Spent fuel modeling and simulation for advanced nda instrument testing in sweden. *TBD*, 2016.